Applied Geochemistry 67 (2016) 153–167

Contents lists available at ScienceDirect

Applied Geochemistry

journal homepage: www.elsevier.com/locate/apgeochem

Trace element mobility in mine waters from granitic pegmatite U–Th–REE deposits, Bancroft area, Ontario

A.J. Desbarats*, J.B. Percival, K.E. Venance

Geological Survey of Canada, Natural Resources Canada, 601 Booth St., Ottawa, ON, K1A 0E8, Canada

ARTICLE INFO

Article history:
Received 25 September 2015
Received in revised form
9 February 2016
Accepted 18 February 2016
Available online 21 February 2016

Keywords:
Uranium
Thorium
Radionuclides
REE
Groundwater

ABSTRACT

Small, low-grade, granitic pegmatite U–Th–REE deposits are found throughout the Grenville geological province of eastern Canada. Groundwater quality at historical mining properties in the Bancroft area was investigated in order to better understand the mobility of trace elements that may pose health risks if there is renewed development of this class of mineral deposit. Groundwater samples were obtained from diamond drill holes, flowing adits and flooded mine shafts. Uranium occurs almost entirely in the dissolved (<0.45 μm) phase and is found at concentrations reaching 2579 μg/L. The Canadian maximum acceptable concentration for U in drinking water (0.02 mg/L) was exceeded in 70% of samples. Regulatory limits for ^{226}Ra (0.5 Bq/L) and for ^{210}Pb (0.2 Bq/L) were generally exceeded in these samples as well. Speciation modeling indicates that over 98% of dissolved U is in the form of highly mobile uranyl-Ca–carbonate complexes known to inhibit U adsorption. Uranium concentrations in groundwater appear to be correlated with the uranothorite content of the deposits rather than with their U grade. Uranothorite may be more soluble than uraninite, the other ore mineral, because of its non-ideal composition and metamict structure. Thorium, released concomitantly with U during the dissolution of uranothorite and thorian uraninite, exhibits median and maximum total concentrations of only 0.1 and 11 μg/L, respectively. Mass balance and stoichiometric considerations indicate that almost all Th is immobilized very close to its source. The sums of total light REE (La–Gd) concentrations have median and maximum values of 6 and 117 μg/L, respectively. The sums of total heavy REE (Tb–Lu) concentrations have median and maximum values of 0.8 and 21 μg/L, respectively. Light REE are derived mainly from the dissolution of metamict allanite whereas the sources of heavy REE are widely dispersed among accessory minerals. Fractionation patterns of REE in the dissolved phase are flat or concave, with negative Ce anomalies associated with more oxic groundwaters. The data suggest preferential LREE and HREE complexation with organic and carbonate ligands in the dissolved phase, respectively. Fractionation patterns in the suspended particulate phase exhibit decreasing enrichment with atomic number from La to Gd and a flat profile from Tb to Lu. This is explained by preferential sorption of LREE and uniform sorption of HREE. Manganese particulates are the most likely sorbents. Potential health risks from Th or REE in mine waters are unlikely due to the very low mobility of these elements. Uranium, on the other hand, exhibits high mobility in shallow, oxic groundwaters and drainage from some mine adits may require mitigation.

1. Introduction

Granitic pegmatite-hosted uranium–thorium–rare earth element (U–Th–REE) deposits and related metasomatic and hydrothermal vein deposits (Rogers et al., 1978) are widely distributed within the Grenville geological province of eastern Canada which includes parts of Ontario, Québec and Labrador (Lentz, 1991, 1996). However, mining of these deposits has been limited to the Bancroft district of southeastern Ontario (Satterly, 1957; Alexander, 1986; Griffith, 1986). Because of their generally low grade and small size, they currently do not present attractive targets for development. Nonetheless, recent spikes in the price of uranium and increased interest in REE has prompted renewed exploration for this class of deposits and the reappraisal of historical prospects. Because they are found relatively close to population centers of southern Canada, public perception of risk associated with exploration and development activities has been more acute. In order to

* Corresponding author.
E-mail address: Alexandre.Desbarats@canada.ca (A.J. Desbarats).

http://dx.doi.org/10.1016/j.apgeochem.2016.02.010
0883-2927/

better inform the debate on uranium exploration, government policy, and regulatory decision-making, there is a need for independent science-based understanding of the geoenvironmental characteristics of granitic pegmatite U–Th–REE deposits. A retrospective investigation of environmental impacts from historical mining activity in the Bancroft district provides a means of acquiring the knowledge required by regulators and proponents to anticipate and mitigate environmental risks associated with the development of new mining projects in similar geological settings.

Impacts to groundwater quality are uppermost among public concerns related to uranium exploration and mining as groundwater is the sole source of potable supply for most rural inhabitants. The principal contaminants of concern associated with the granitic pegmatite-hosted U–Th–REE deposits of the Bancroft district are U, Th and their radioactive decay products. Although the health risks from REE in drinking water are not yet well understood (EPA, 2012; Pagano et al., 2015), REE are also of interest here because this class of deposits provides a useful proxy for as-yet unmined peralkaline rock REE deposits in more remote parts of Canada (Richardson and Birkett, 1996).

Naturally occurring U is a radioactive heavy metal composed mainly of the isotope ^{238}U. Because of the long half-life of ^{238}U, the radioactivity of natural U is low and its potential health effects relate more to its chemical toxicity as a heavy metal (Health Canada, 2001). While most U ingested through drinking water is eliminated from the body, the small amount that is absorbed into the bloodstream can cause damage to kidney cells. In Canada, the maximum acceptable concentration (MAC) of U in drinking water is 0.02 mg/L (Health Canada, 2014). Radioactive decay of ^{238}U produces daughter products which may also represent environmental concerns. Of these products, the radionuclides radium-226 (^{226}Ra), radon-222 (^{222}Rn) and lead-210 (^{210}Pb) pose the greatest potential hazard to human health. Both ^{226}Ra and ^{210}Pb are absorbed in the gastrointestinal track and are associated with increased risks of leukemia and cancers of the lung, breast, thyroid, bone, digestive organs and skin (Health Canada, 2010). Maximum acceptable concentrations of ^{226}Ra and ^{210}Pb in drinking water are 0.5 and 0.2 Bq/L, respectively (Health Canada, 2010). Radon-222 is a gas, highly soluble in groundwater, linked to an increased risk of lung cancer if inhaled. However, because of its high volatility it presents a negligible health risk from ingestion and no maximum acceptable concentration in drinking water is necessary (Health Canada, 2014).

Naturally occurring Th is a radioactive heavy metal composed mainly of the isotope ^{232}Th which has a 14 billion year half-life and therefore a very slow decay rate. Thorium-232 is extremely insoluble and is not readily mobilized in groundwater (Cothern and Rebers, 1990). Decay products of ^{232}Th include radium-228 (^{228}Ra) and radium-224 (^{224}Ra). Because of its relatively short half-life compared to groundwater travel times and the insolubility of its parent, ^{228}Ra is not readily dispersed far from its source. Radium-224 is a decay product of ^{228}Ra and their concentrations in groundwater tend to be well-correlated (Focazio et al., 2001). Most Th ingested through drinking water is rapidly excreted from the body. However, the remaining amount may accumulate in the bones and pose a risk for bone cancer. The health effects for short- and long-term exposure of humans to drinking water containing specific levels of Th are not well understood (ATSDR, 1990). There are currently no drinking water standards for Th in Canada.

Unmineralized granitic rocks are often enriched in U and potential effects on groundwater quality have been widely investigated (Gascoyne, 1989; Lahermo and Juntunen, 1991; Banks et al., 1995; Ayotte et al., 2007; Vinson et al., 2009; Warner et al., 2011; Prat et al., 2009; Yang et al., 2014; Krall et al., 2015). Risks to groundwater quality from granite-hosted U deposits, whether undeveloped (Jerden and Sinha, 2003; Gannon et al., 2012) or developed (Gomez et al., 2006), have received less attention. As part of a regional survey of U in surface waters of the Bancroft mining camp, Chamberlain (1964) observed that anomalously high concentrations in waters associated with mine development generally decreased to near-background values within a few hundred feet of their source. Downstream mobilization of U appears to have been limited by reductive precipitation promoted by decaying organic matter in surface water drainages. Generally, however, mining activities tend to enhance water-rock reactions and U mobilization over greater distances downstream (Wanty et al., 1999; Campbell et al., 2015).

This study examines the groundwater geochemistry of trace elements from granitic pegmatite U–Th–REE deposits in near-field settings ranging from undeveloped prospects to past-producing mines. Scales of observation range from exploration boreholes to flowing adits and flooded mine shafts. The objectives of the study are to address the following questions:

1. What is the trace element signature of U–Th–REE deposits in drainage from historical exploration prospects and mines?
2. What are the geological factors and the geochemical processes that control the release and mobility of species of interest in the near-field mine environment?

The groundwater chemistries of U and its daughter products, Th and REE are reviewed and factors controlling their mobilities are assessed. Geochemical inverse modeling (Plummer et al., 1983; Alpers and Nordstrom, 1999) of drainage chemistry from five exploration adits is then used to show how key factors controlling trace element mobility are determined by weathering reactions affecting ore minerals and their host rocks.

Other important questions concern the baseline trace element signature in groundwater from surrounding unmineralized bedrock and the downstream persistence of trace element concentrations in mine waters discharged to surface water drainages. These are addressed in a companion report (Desbarats and Percival, 2016).

2. Site description

2.1. Physiographic and climatic setting

The study area (Fig. 1) is located in southeastern Ontario, approximately 250 km west of Ottawa. The area's bedrock forms broad uplands and lowlands with elevations ranging between 343 and 500 m. The strongly glaciated landscape is characterized by ridged or hummocky outcrops covered with thin, discontinuous till in the uplands, and large areas of glaciofluvial and lacustrine deposits in the lowlands. Drainage patterns are controlled by bedrock lithology and structure. Higher-order radial and concentric drainage networks are developed on low-permeability plutonic domes which form the main uplands. These feed the larger lakes and meandering rivers found in lowlands associated with more recessive metasedimentary and metavolcanic rocks that ring the domal structures. Numerous wetlands include small bogs formed in upland depressions and large marshes bordering rivers in the lowlands.

The study area lies within a Humid-High-Cool-Temperate ecoclimatic region characterized by warm summers and cold winters (Strong et al., 1989). At Haliburton (Lat. 45.0322° N; Lon. 78.5311° W; Elev. 330 m), the nearest active weather station, the mean annual temperature is approximately 5.0 °C. The mean summer (July) temperature is 18.7 °C and the mean winter (January) temperature is −9.9°. Mean annual precipitation is approximately 1074 mm including 794 mm of rainfall and 280 mm of snowfall

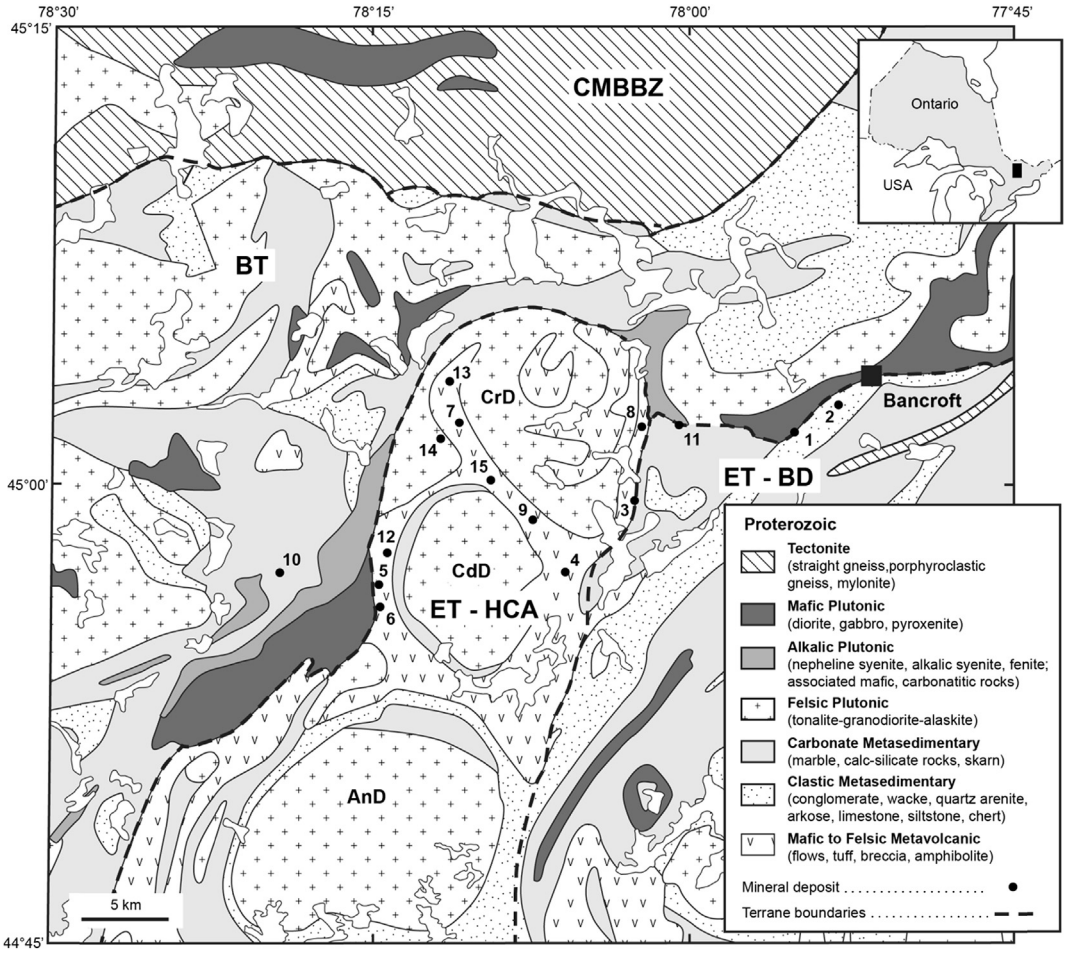

Fig. 1. Simplified geological map of the study area showing locations of past producing U mines and selected prospects; (CMBBZ) Central Metasedimentary Belt Boundary Zone; (BT) Bancroft Terrane; (ET-BD) Belmont Domain of the Elzevir Terrane; (ET-HCA) Harvey-Cardiff Arch of the Elzevir Terrane; (AnD) Anstruther Dome; (CdD) Cheddar Dome; (CrD) Cardiff Dome; (1) Madawaska Mine; (2) Greyhawk Mine; (3) Bicroft Mine; (4) Dyno Mine; (5) Amalgamated Rare Earth No. 1 Mine; (6) Amalgamated Rare Earth No. 2 Mine; (7) Halo Mine; (8) Croft Mine; (9) Canada Radium Mine; (10) Canadian All Metals Mine; (11) Silver Crater Mine; (12) Saranac Prospect; (13) Richardson-Fission Mine; (14) Cardiff Mine; (15) Kenmac-Chibougamau Mine. Map modified from OGS (1991).

equivalent (Environment Canada, 2014a).

2.2. Geological setting

The Bancroft mining camp is located within the Central Metasedimentary Belt (CMB) of the Proterozoic Grenville Province, a complex (ca. 1100 Ma) orogenic belt truncating older geological provinces. Bordered to the northwest by tectonite rocks of the Central Metasedimentary Belt Boundary Zone (CMBBZ), the CMB is subdivided into a succession of allochthonous terranes extending to the southeast (Easton, 1992). The study area lies immediately south of the CMBBZ, in the Bancroft Terrane and in adjacent parts of the Harvey-Cardiff Arch Domain of the Elzevir Terrane (Fig. 1).

The CMB represents a major Mid-Proterozoic accumulation of supracrustal rocks intruded by compositionally diverse plutonic rocks metamorphosed at grades from greenschist to granulite facies (Easton, 1992). The (1400–1250 Ma) supracrustal deposits of the Bancroft Terrane consist mainly of marbles with quartz arenite, feldspathic gneiss and minor metavolcaniclastic rocks of shallow marine origin. In the Harvey-Cardiff Arch, the (1300–1250 Ma) supracrustal rocks include metavolcanics, metawackes, metapelites and turbidites reflecting a deeper active basin setting (Easton, 1992). These rocks have been intruded by a succession of major plutonic suites (Easton, 1992). The (1290–1250 Ma) Nepheline Syenite Suite forms discontinuous belts of small elongated sills in the Bancroft Terrane (Lumbers et al., 1990; Easton, 1992). Plutons of the (1280–1270 Ma) "Elzevir" Tonalite Suite and the (1250–1240 Ma) "Methuen" Alaskite Suite form the Anstruther, Cheddar and Cardiff gneiss domes of the Harvey-Cardiff Arch (Fig. 1). Uranium mineralization is associated with the (1070–1040 Ma) Fenite-Carbonatite and (1050–1030 Ma) Granite Pegmatite post-tectonic plutonic events. The fenites and carbonatites occur in a band running the length of the Bancroft Terrane paralleling the CMBBZ (Easton, 1992) and overlapping the earlier Nepheline Syenite Suite. The related pegmatites occur as long, narrow dykes in the metasedimentary and metavolcanic rocks flanking the plutonic domes of the Harvey-Cardiff Arch. They are also common within the fenite-carbonatite belt.

The temporal, spatial and geochemical relationship among the granitic pegmatites, fenites and carbonatites hosting U, Th and REE mineralization suggests that they share a common magmatic hydrothermal origin (Lumbers et al., 1990; Lentz, 1991, 1996). Satterly (1957) and Lentz (1991) have classified U–Th–REE deposits of the CMB into mineralogically-complex pegmatites, metasomatic skarns and hydrothermal calcite veins. As a result of their related genesis, many deposits of the study area exhibit characteristics of more than one type, such as pegmatite-skarn or pegmatite-calcite vein.

Complex pegmatites occur as both intrusive and replacement

bodies, with varying degrees of host-rock assimilation. Their mineralogical complexity arises from metasomatic hybridization of simple pegmatites with host rocks of varying composition (Lentz, 1996 and references therein). The pegmatites usually consist of quartz, perthite, plagioclase, biotite, Ca-pyroxene, and Na-hornblende. Accessory minerals include calcite, fluorite, apatite, magnetite, pyrite and molybdenite. Uranium and Th minerals consist mainly of disseminated uraninite and uranothorite. Rare Earth Element-bearing minerals include allanite, euxenite, cyrtolite, bastnaesite and fergusonite (Satterly, 1957; Sabina, 1986; Lentz, 1991; Easton and Fyon, 1992; Lentz, 1996). Uranium and REE enrichment is associated with a greater degree of pegmatite hybridization with mafic host rocks (Satterly, 1957; Easton and Fyon, 1992; Lentz, 1996).

Uraniferous skarns form lenticular or irregular bodies occurring as marginal zones of granitic pegmatites, as replacement zones, and as veins (Lentz, 1991). Marble-hosted skarns contain silica-rich assemblages of calcite, diopside, tremolite, phlogopite and sulfides (Satterly, 1957; Lentz, 1991). Metapyroxenite-hosted skarns, in amphibolites and marbles intruded by syenitic or granitic bodies, are composed of pyroxene and mica with accessory apatite, scapolite, titanite and fluorite (Satterly, 1957; Lentz, 1991). Uranium mineralization is erratic and consists of disseminated uraninite and uranothorite (Satterly, 1957).

Uraniferous hydrothermal calcite veins occur in shear zones and along geological contacts as discontinuous, lenticular fissure-fillings. In addition to calcite, principal vein minerals include fluorite, apatite, biotite and pyrite. Diopside, amphibole, biotite, feldspar, titanite and uranium-bearing minerals occur along vein selvages (Lentz, 1991). Generally, selvage composition depends on host-rock composition and may be similar to that of related skarns (Lentz, 1991; Easton and Fyon, 1992). Uranium-bearing minerals consist of uraninite, uranothorite and betafite (Satterly, 1957). The presence of biotite appears to be an important control on the localization of mineralization (Satterly, 1957).

2.3. Sampling locations

Hewitt (1967) and Gordon et al. (1981) provide an exhaustive list of U–Th–REE occurrences in Faraday, Cardiff and Monmouth townships west of Bancroft. Field work objectives were to sample groundwater from as many of these occurrences as possible subject to operational and safety considerations. Groundwater from some important deposits could not be sampled because access was denied by the property owner. In other cases, recent site restoration activities rendered groundwater inaccessible to sampling. A number of lesser occurrences could not be located due to the passage of time since exploration activities occurred. Depending on the extent of mining development at each site, groundwater samples were obtained from flooded shafts, flowing adits, and diamond drill holes (DDH). Table 1 presents a list of sampled sites along with the number and sources of samples at each site. Over the three year study period, a total of 41 samples including 8 duplicates were obtained from 10 different mine sites and one stream. Locations of the sites are shown in Fig. 1.

3. Methods

3.1. Field procedures

Groundwater sampling was carried out from September 27 to October 5 in 2011, from September 11 to September 20 in 2012, and from August 21 to August 29 in 2013. Sampling was performed in late summer or early autumn, near the end of the hydrological year (September 30) when groundwater dilution by recharge from snowmelt is minimal.

Groundwater samples from flooded shafts and flowing adits were collected using a peristaltic pump whereas samples from DDH were taken using a submersible pump. The pumps discharged to flow cells. Each DDH was purged for 20 min and allowed to recover for another 20 min. This cycle was repeated two or three times in order to ensure clear flow and stabilized field measurements prior to sampling from the flow cell. Generally, water levels recovered fully between purges suggesting that host rocks have a relatively high fracture-controlled permeability.

The groundwater pH instrument was calibrated daily over the 7–10 range. The Specific Conductance (SC) instrument was calibrated daily over the 0 to 1413 μS/cm range. Temperature was also measured using the SC meter. Field parameters were recorded once values had stabilized in the flow cell.

Groundwater was sampled from flow cells using all-plastic 50 mL syringes triple-rinsed in the water to be sampled. Unfiltered samples for (total) cations were collected in triple-rinsed 60 mL HDPE bottles. Filtered (<0.45 μm) samples for anions and cations were also collected in triple-rinsed 60 mL HDPE bottles. At each mine site, one filtered (<0.45 μm) sample for radio-isotopes (^{226}Ra, ^{210}Pb) was collected in a triple-rinsed 1-L HDPE bottle, usually from an adit or shaft if present. Bottles for cation samples were acidified immediately in the field to pH < 2 by adding 0.5 mL of 8 N ultrapure nitric acid. The 1-L samples for radio-isotopes were acidified with ultrapure nitric acid upon return to the Geological Survey of Canada in Ottawa before being sent to a commercial laboratory for analysis. Duplicate water samples were collected every tenth sample, and travel blanks, acid blanks, and sample blanks were prepared once per two-week field program. Samples were stored at 4 °C pending shipment to the laboratory.

3.2. Laboratory methods

All groundwater samples were analyzed for standard chemical and physical parameters at the Inorganic Geochemical Research Laboratory of the Geological Survey of Canada in Ottawa. Analyses of major elements were performed by Inductively Coupled Plasma–Atomic Emission Spectroscopy (ICP–AES) using a Perkin–Elmer 3000 DV. Analyses of trace elements were performed using Inductively Coupled Plasma–Mass Spectrometry (ICP–MS) with a Thermo Corporation X-7 Series II. Determinations of anion concentrations were made with a Dionex DX-600 ion chromatograph using an AS-18 column and gradient elution. Alkalinities were determined using a PC-Titrate System. For each sample batch, analyses were performed on one or more certified standards of known concentrations. Analytical results for field blanks from each trip were at or below detection limits for all elements. Analyses for Th were unavailable in 2011. Charge balance errors varied between −6.18% and 4.26% with a mean value of −0.35%.

Selected groundwater samples from each field site were analyzed for Ra-226 and Pb-210 by Becquerel Laboratories Inc. of Mississauga, Ontario. Analyses for ^{210}Pb were performed by gross beta count (Gas Flow Proportional Counting) with a detection limit of 0.2 Bq/L. Analyses for ^{226}Ra were performed by alpha particle spectrometry with a detection limit of 0.01 Bq/L.

Electron microprobe analyses of mineral samples were acquired at University of Ottawa on a JEOL 8230 EPMA fitted with 5 wavelength-dispersive spectrometers with a take-off angle of 40°. Operating conditions were 20 kV accelerating voltage and 20 nA current. Standards used were a mix of synthetic and natural minerals. Data reduction was accomplished with a ZAF matrix correction (Armstrong, 1988).

Table 1
List of water sampling sites.

U–Th–REE occurrence	Longitude (west)	Latitude (north)	Geology	Sample source and number of samples
Bicroft mine	78.033	44.994	Pegmatite intruding amphibolite, paragneiss	Shaft (1)
Amalgamated rare earth mines no. 1	78.252	44.953	Pegmatite intruding quartzite, marble, amphibolite	Adit (1)
Amalgamated rare earth mines no. 2	78.247	44.934	Pegmatite intruding metagabbro, amphibolite	Adit (3); DDH (2)
Halo mine	78.178	45.028	Pegmatite and calcite veins intruding amphibolite, paragneiss, marble, pyroxenite	Adits (2); DDH (2)
Croft mine	78.030	45.033	Pegmatite intruding amphibolite, paragneiss	Adit (3); DDH (15); Stream (1)
Croft south zone prospect	78.033	45.006	Pegmatite intruding amphibolite, paragneiss	DDH (3)
Canada radium mine	78.130	44.986	Pegmatite intruding amphibolite, paragneiss, marble	Shaft (1)
Canadian all metals mine	78.323	44.947	Silicated marble skarn within marble, quartzite, paragneiss	DDH (3)
Silver crater mine	78.010	45.029	Carbonatite sill intruding syenitic gneiss, biotite-hornblende gneiss	Adit (1); DDH (2)
Saranac east prospect	78.241	44.962	Pegmatite intruding hornblende gneiss	DDH (1)

3.3. Speciation modeling

Speciation modeling of groundwater chemistry and the calculation of mineral saturation indices (SI) were performed using PHREEQC version 2.8 (Parkhurst and Appelo, 1999) with the WATEQ4F thermodynamic database (Ball and Nordstrom, 1991). Thermodynamic data for coffinite–uranothorite–thorite minerals were obtained from Szenknecht et al. (2013) and from Langmuir and Herman (1980) for Th species. Thermodynamic data for ternary uranyl-calcium–carbonato complexes were obtained from Dong and Brooks (2006, 2008). PHREEQC was also used for inverse modeling.

4. Results and discussion

4.1. Field parameters and major dissolved species

The specific conductance (SC) of groundwaters associated with the spectrum of U–Th–REE deposits varies between 171 and 980 μS/cm. Values depend on the reactivity of host-rocks, on water-rock contact time, and on water-rock contact area. The highest values are associated with silicate host-rocks and are observed in samples from deep DDH and from the shaft of the flooded Bicroft mine. Groundwaters associated with marble skarn deposits and carbonatites exhibit intermediate (circa 400 μS/cm) SC values, possibly controlled by calcite solubility. Lower values are associated with shorter groundwater contact times in silicate host-rocks. The pH of groundwaters varies between 6.43 and 8.17. The highest values are associated with the weathering of silicate-hosted deposits. Values in the range of 7.5–7.9 reflect groundwaters in equilibrium with calcite. The lowest values are associated with shallow groundwaters of recent meteoric origin. Although Eh was not measured in the field, an Eh value for the Fe(III)/Fe(II) redox couple was estimated from pH and dissolved Fe assuming equilibrium with amorphous $Fe(OH)_3$ (Hem and Cropper, 1959). Calculated Eh for groundwaters ranges between 11 and 342 mV. Corresponding p*e* values vary between 0.19 and 6.12.

The cation chemistry of groundwaters from U–Th–REE deposits is dominated by Ca (Fig. 2a). Calcite is a ubiquitous accessory mineral in these deposits (Satterly, 1957) although some Ca is derived also from the weathering of amphiboles, pyroxenes and plagioclase. The Mg content of groundwaters is derived mainly from ferromagnesian silicate minerals. Indeed, the highest Mg fractions are encountered in DDH tapping the metagabbro of the Amalgamated Rare Earth No. 2 deposit. The Na and K content of groundwaters mainly reflect weathering of albite and biotite, respectively. The highest fractions of these species are associated with long residence times as encountered in samples from deep DDH.

The anion chemistry of groundwaters is dominated by HCO_3 (Fig. 2b) although SO_4 derived from sulfide (mainly pyrite and molybdenite) oxidation is significant in some samples from deep DDH at the Croft and Halo sites. Anomalous Cl concentrations are observed in shallow groundwaters sampled in two DDH adjacent to a highway (Croft South Zone). These samples are believed to reflect contamination by road de-icing salt.

Speciation modeling results indicate that groundwaters associated with silicate-hosted deposits are over-saturated with respect to K-feldspar (microcline), under-saturated with respect to albite, biotite (phlogopite), amphibole (tremolite) and in equilibrium with respect to chalcedony (SiO_2). Groundwaters from adits or flooded shafts are at or near saturation with respect to calcite whereas groundwaters from DDH samples exhibit varying degrees of undersaturation.

4.2. Common metals

The partitioning of common metals (Al, Mn, Fe) between dissolved and particulate phases is of interest because their precipitates are potential sorbents of trace elements. Operationally, dissolved concentrations are defined here as filtered values. Suspended particulate (P) concentrations are defined as the difference between total (T) and filtered (F) values.

Aluminum, derived from silicate dissolution, occurs mainly in the suspended particulate phase (Fig. 3). Speciation modeling results show that groundwaters are under-saturated with respect to amorphous $Al(OH)_3$ ($-2.1 < SI < -0.2$) and over-saturated with respect to gibbsite ($0.33 < SI < 2.17$) suggesting equilibrium with a poorly crystalline $Al(OH)_3$ phase.

Manganese, derived mainly from the dissolution of amphibole and biotite, occurs in both the dissolved and particulate phases (Fig. 3). Speciation modeling results show that all groundwaters are highly under-saturated with respect to ideal birnessite or manganite. The nature of the particulate Mn phase is unclear although it is possibly poorly crystallized birnessite (Parc et al., 1989).

Iron is derived mainly from the dissolution of ferro-magnesian silicates, with a minor contribution from Fe sulfides. It occurs largely in the particulate (>0.45 μm) phase with two notable exceptions (Fig. 3). Very high dissolved Fe concentrations are observed in samples from the flooded shaft of the Canada Radium Mine (pe = 0.42) and from a flowing DDH at the Halo Mine site (pe = 1.80). Speciation modeling results show that all groundwaters are in equilibrium ($-0.03 < SI < 0.44$) with respect to amorphous $Fe(OH)_3$.

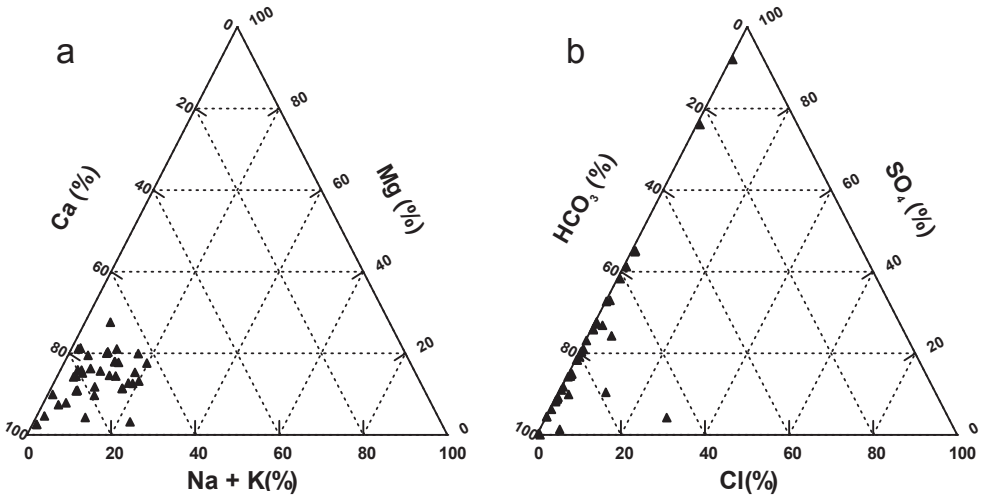

Fig. 2. Ternary plots of major dissolved species (in meq/L): (a) cations; (b) anions.

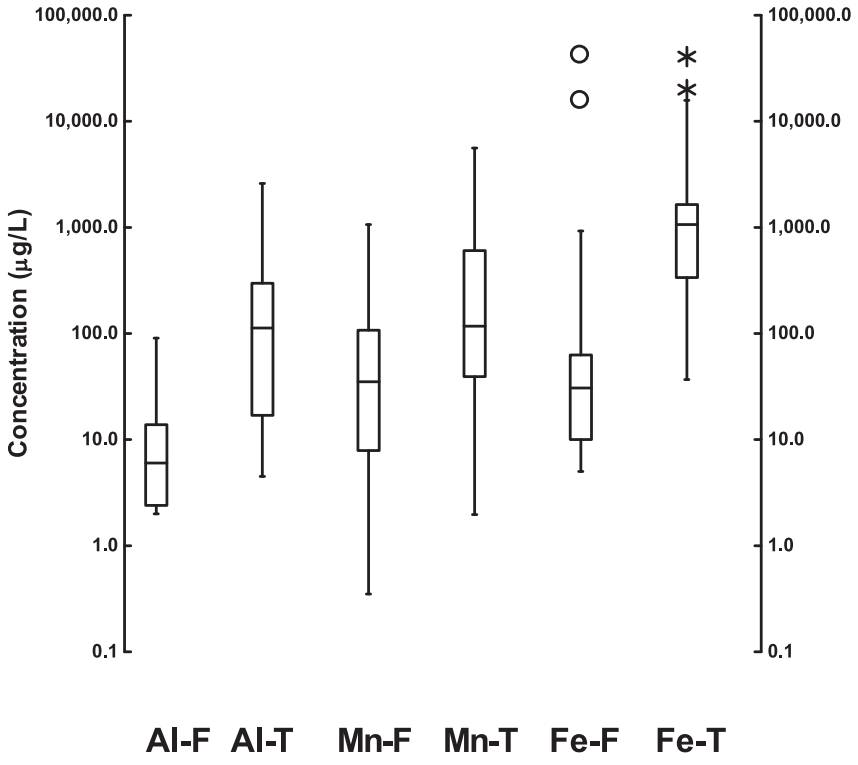

Fig. 3. Box plots showing the distributions of filtered (F) and total (T) concentrations of Al, Mn and Fe in groundwaters. Particulate concentrations are defined as the difference between total and filtered values.

4.3. Trace elements and radionuclides

The statistical distributions of trace element concentrations in groundwaters from U–Th–REE deposits (Fig. 4 and Table 2) show that U occurs almost entirely in the dissolved phase and at relatively high concentrations. Concentrations of Th and REEs are very much lower and these species occur primarily in the particulate phase. Sources of trace elements and controls on their mobility in groundwater are reviewed below.

4.3.1. Uranium and daughter products

In the Bancroft mining camp, the main U-bearing minerals are uraninite and uranothorite. While uraninite was the most important ore mineral, uranothorite also contributed to U grades and was the dominant U mineral in a number of unmined prospects. Average ore grades at the former Madawaska, Bicroft, Dyno and Greyhawk mines were 0.099, 0.086, 0.093 and 0.076% U_3O_8, respectively (Alexander, 1986; Gordon et al., 1981; Griffith, 1986).

Uraninite has an ideal composition of UO_2. However, in most natural uraninite, U(IV) may be partially oxidized to U(VI) and REE and cation substitutions may occur in the mineral structure yielding compositions of the form $U^{4+}_{1-x-y-z}\ U^{6+}_{x}\ REE^{3+}_{y}\ M^{2+}_{z}\ O_{2+x-y-z}$ (Janezcek and Ewing, 1992). Bancroft uraninites also contain variable amounts of Th and radiogenic Pb (Robinson and

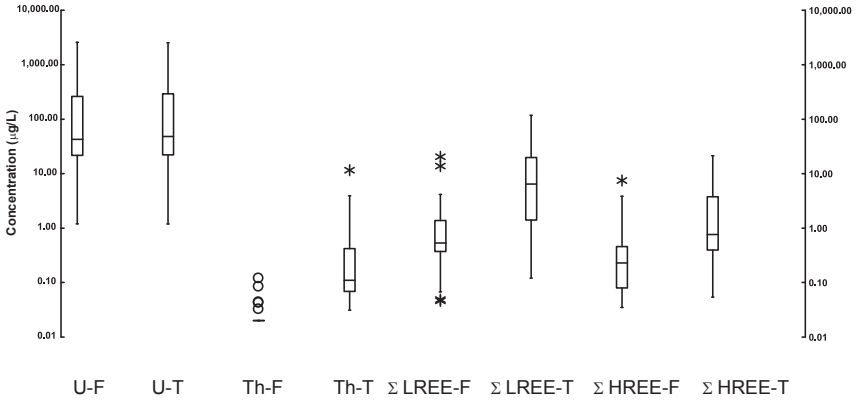

Fig. 4. Box plots showing the distributions of filtered (F) and total (T) concentrations of U, Th, sum of light REE (La–Gd), and sum of heavy REE (Tb–Lu).

Table 2
Summary statistics for filtered (F) and total (T) trace element concentrations (µg/L).

	U–F	U–T	Th–F	Th–T	Σ LREE-F	Σ LREE-T	Σ HREE-F	Σ HREE-T
n	41	41	28	28	41	41	41	41
Minimum	0.6	1.2	0.02	0.03	0.05	0.12	0.03	0.05
Maximum	2579	2530	0.12	11.5	20.4	117.4	7.5	21.3
Median	40.7	48.1	0.02	0.1	0.5	6.2	0.2	0.8
Mean	203	214	0.03	0.8	1.7	14.1	0.6	2.7

Sabina, 1955). Uranothorite, with an ideal composition of $(Th^{4+}_{1-x}U^{4+}_{x})SiO_4$, forms a solid solution between Th and U end-members, thorite and coffinite. Bancroft uranothorites have an approximate ideal composition of $(Th_{0.8}U_{0.2})SiO_4$. However, they are usually metamict and contain Ca, Fe, REE, H_2O, and radiogenic Pb (Robinson and Abbey, 1957).

Speciation modeling results indicate that all mine waters are under-saturated with respect to uraninite and coffinite although they are over-saturated with respect to $(Th_{0.8}U_{0.2})SiO_4$ and thorite. As a solid solution, however, uranothorite should dissolve more readily than either of its end members, coffinite and thorite (Szenknecht et al., 2013). Thus, modeling results based on the thermodynamic data of Szenknecht et al. (2013) appear to contradict field observations of elevated U concentrations in groundwater associated with deposits where uranothorite is the main ore mineral. It is likely that the non-ideal composition and metamict structure of uranothorite may enhance its solubility (Warner et al., 2011; Krall et al., 2015).

Oxidation and dissolution of both uraninite and uranothorite yields U(VI) which is more mobile than U(IV) in most groundwater environments. The dominant aqueous form of U(VI) depends on pH and on the concentrations of complexing agents such as phosphate or carbonate ions (Grandstaff, 1976; Langmuir, 1978; De Pablo et al., 1999) and calcium and magnesium (Bernhard et al., 1996; Kelly et al., 2007). Although apatite is an accessory mineral in some Bancroft area deposits, phosphate concentrations are negligible. Speciation modeling results (Fig. 5) suggest that ternary uranyl-Ca–carbonate complexes are the main U(VI) species in mine waters from granitic pegmatite and related U–Th–REE deposits. Together, $Ca_2UO_2(CO_3)_3$ and $CaUO_2(CO_3)_3^{2-}$ represent over 98% of U in solution. This result is consistent with other reports of the dominance of uranyl-Ca–carbonate complexes in natural circum-neutral groundwater settings (Prat et al., 2009). Activities of all three uranyl tri-carbonato complexes increase with pH up to a maximum at pH = 7.5 and decrease thereafter (Fig. 5). This decrease may be caused by a decrease in Ca available for complexation due to calcite precipitation. The pH dependence and activities of Mg $UO_2(CO_3)_3^{2-}$

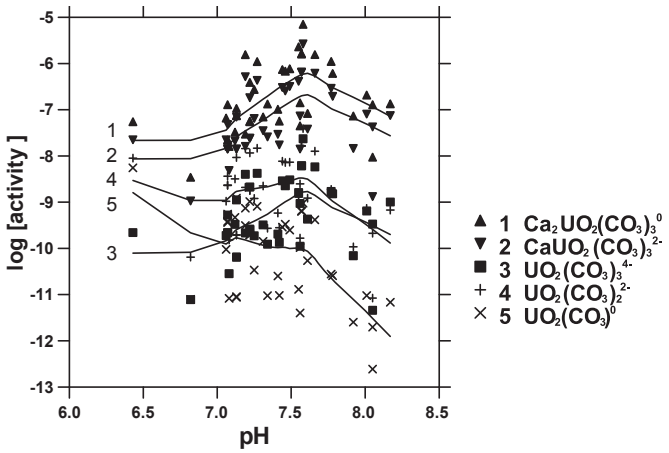

Fig. 5. Calculated activities of the principal uranyl–carbonate and uranyl–calcium–carbonate complexes in mine waters as a function of pH. The solid lines represent moving averages for each complex.

complexes (not shown) are similar to those of $UO_2(CO_3)_3^{4-}$.

Precipitation of secondary uranyl minerals is unlikely to affect U mobility in Bancroft area mine waters: At ambient pH values and in the presence of high concentrations of P or V, uranyl-phosphate or uranyl-vanadate minerals could precipitate (Langmuir, 1978; Jerden and Sinha, 2003); however P and V concentrations are at or below their detection limits. Precipitation of schoepite or uranophane is unlikely as speciation modeling shows that groundwaters are highly under-saturated with respect to these phases. Reduction of U(VI) complexes and precipitation of amorphous uraninite does not appear likely based on speciation modeling results as all samples are highly under-saturated (SI < −3.4) with respect to amorphous UO_2. Some research suggests that bioreduction of U(VI) is inhibited by the formation of uranyl-Ca–carbonate complexes (Brooks et al., 2003). Based on the data displayed in Fig. 4, adsorption of U on suspended particulate material is minor. The particulate U fraction

varies between 0 and 73%, of total U with a median value of 3%. It increases with Fe concentration in the particulate phase (not shown). Recent research suggests that adsorption of U on goethite or ferrihydrite may be inhibited by the formation of uranyl-Ca–carbonate complexes under mildly alkaline conditions (Fox et al., 2006; Stewart et al., 2010).

Natural U is composed of the three isotopes ^{238}U (99.28%), ^{235}U (0.72%) and ^{234}U (0.005%) with half-lives of 4468 $\times$ 10^6, 704 $\times$ 10^6, and 247 $\times$ 10^3 years, respectively. In groundwater, U occurs mainly as ^{238}U and as ^{234}U from its decay series. Radioactive decay of ^{238}U creates other daughter products including ^{226}Ra and ^{210}Pb with half-lives of 1620 and 21 years, respectively. As observed by others (Asikainen, 1981; Gascoyne, 1989; Szabo and Zapecza, 1991), there is no strong correlation between the concentration of U and the activity of ^{226}Ra (Fig. 6a). This is because of the different mobilities of these species in the groundwater environment and because U and ^{226}Ra are separated in the ^{238}U decay series by the long-lived and almost insoluble isotope ^{230}Th (Gascoyne, 1989; Wanty and Schoen, 1991). If U concentration is expressed as an equivalent activity of ^{238}U (1 μg/L = 12.437 $\times$ 10^{-3} Bq/L), the activity ratio ^{238}U/^{226}Ra ranges between 0.06 and 29.17 and has a median value of 2.4. Similar degrees of radioactive disequilibrium were observed by Asikainen (1981). A plot of p*e* versus ^{238}U/^{226}Ra (Fig. S.1a, Supplementary Information) indicates that U is preferentially mobilized in more oxic groundwaters whereas ^{226}Ra is dominant under more reducing conditions. This is consistent with the observations of Gascoyne (1989) and Szabo and Zapecza (1991).

The plot of U versus ^{210}Pb (Fig. 6b) does not suggest any simple correlation between these species either. However, a plot of ^{210}Pb versus ^{226}Ra (not shown) reveals a moderate correlation ($r^2 = 0.68$; $n = 17$) between the activities of these decay products. This suggests a greater degree of equilibrium between radionuclides separated by relatively short-lived isotopes in the ^{238}U decay chain. The activity ratio ^{238}U/^{210}Pb ranges between 0.15 and 46.18 and has a median value of 2.1. A plot of p*e* versus ^{238}U/^{210}Pb (not shown) does not show any relationship between the activity ratio and redox conditions. However, a plot of p*e* versus ^{226}Ra/^{210}Pb (Fig. S.1b, Supplementary Information) suggests that ^{226}Ra is more mobile than ^{210}Pb under more reducing conditions.

Although correlations between U and ^{226}Ra and ^{210}Pb are weak, the data in Fig. 6 suggest that groundwaters exhibiting U concentrations greater than the Health Canada (2014) maximum acceptable concentration of 20 μg/L are also likely to exhibit ^{226}Ra and ^{210}Pb levels in excess of regulatory limits.

4.3.2. Thorium

In Bancroft area deposits, uranothorite is the principal mineral in which Th occurs as a major constituent. However, Th is also a minor constituent in local uraninites as discussed above, and it occurs in a host of exotic minerals identified in Bancroft area deposits including cyrtolite, euxenite and monazite (Sabina, 1986).

Most thorium-bearing minerals are refractory to weathering and Th is considered essentially insoluble in most natural waters (Wanty and Schoen, 1991). Here, however, Th is released along with U from more readily dissolved uranothorite and uraninite. If the dissolution of these minerals releases significant amounts of U, commensurate amounts of Th must be released also. Nonetheless, both dissolved and suspended particulate concentrations of Th are extremely low (Fig. 4). Therefore, these concentrations must reflect effective removal of Th from both the dissolved and suspended particulate phases. It would appear that Th mobility in groundwaters is being limited near source by adsorption to immobile particulates or surfaces in fractures. Thorium may form inorganic and organic complexes which increase the solubility of Th minerals and the mobility of Th in groundwater (Langmuir and Herman, 1980). However, for the conditions observed in this study (low phosphate and DOC concentrations, 6.0 < pH < 8.5), Th is hydrolyzed to $Th(OH)_4^0$ almost entirely and this species is known to sorb strongly on environmental particulates whereupon Th may be immobilized or transported in a colloidal phase (Degueldre and Kline, 2007; Zänker and Hennig, 2014).

Suspended particulate concentrations of Th in groundwaters from Bancroft area deposits are weakly or moderately correlated with particulate concentrations of Al, Fe and Mn suggesting that Th may be sorbed to oxyhydroxides of each these metals (Fig. 7). However, this may be a statistical artefact caused by cross-correlation among Al, Fe and Mn particulate concentrations: a Th correlation with any one of these metals would yield an apparent correlation with the others. Here, based on the lesser degree of data scatter in Fig. 7b, sorption of Th on Fe oxyhydroxides appears most likely.

4.3.3. Rare earth elements

A complete list of REE-bearing minerals identified in granitic pegmatites of the Grenville Province of southeastern Ontario has been compiled by Goad (1990). In addition to such hosts, REE can substitute in the structure of rock forming minerals including hornblende, apatite, feldspar and biotite. Thus, there are numerous possible sources of REE in groundwaters and their relative importance depends on their in-situ abundance and leachability. Bastnaesite, fergusonite and euxenite may be significant REE sources

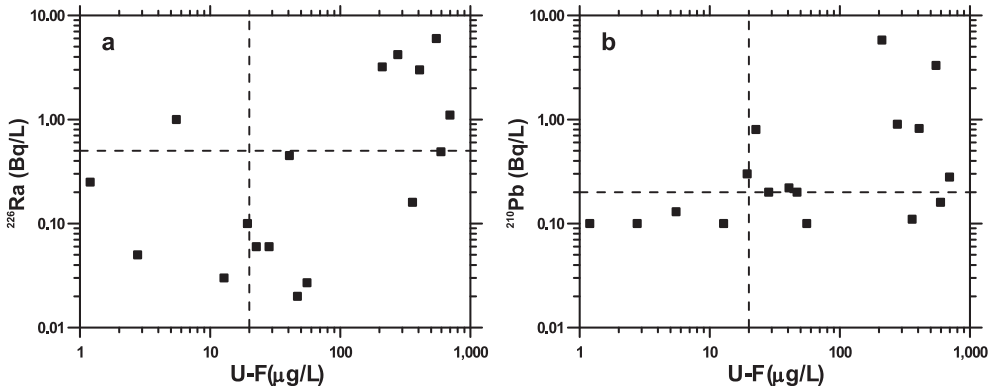

Fig. 6. Relationship between U concentration (filtered) and activities (filtered) of radionuclide daughter products: (a) Ra-226; (b) Pb-210. Dashed lines represent Health Canada (2014) maximum acceptable concentrations or activities for U (20 μg/L), Ra-226 (0.5 Bq/L) and Pb-210 (0.2 Bq/L).

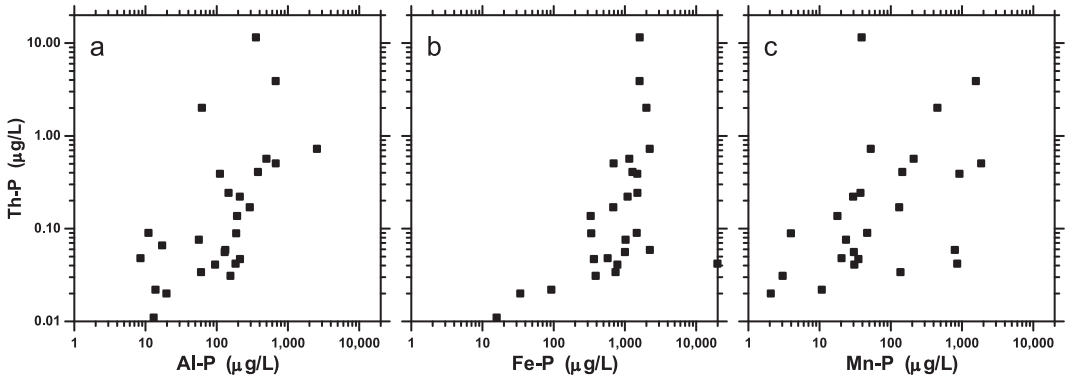

Fig. 7. Adsorption of suspended particulate Th on possible sorbents: (a) particulate Al; (b) particulate Fe; (c) particulate Mn.

locally (Sabina, 1986); however allanite ($(Ce,Ca,Y)_2(Al,Fe)_3(SiO_4)_3(OH)$) is the most common REE-bearing mineral in Bancroft area deposits (Peterson and MacFarlane, 1993). Because of its frequent metamict structure and resulting non-ideal composition (Ercit, 2002), allanite is readily weathered (Price et al., 2005) and is likely the dominant source of REE in mine waters. Allanites from the Bancroft area contain light REE (La–Gd) almost exclusively (Peterson and MacFarlane, 1993).

Chondrite-normalized whole-rock REE fractionation patterns for Grenville granitic pegmatites (Lentz, 1996) are characterized by decreasing enrichment with atomic number over the range of light REE (La–Gd) and a flat profile over the range of heavy REE (Tb–Lu). They also exhibit small negative Eu anomalies but no negative Ce anomalies. Various fractionation processes such as differential weathering of REE-bearing minerals, complexation and adsorption, as well as local pH and redox conditions (Dia et al., 2000; Tang and Johannesson, 2006), have acted on original host-rock compositions and have shaped distinct groundwater REE patterns in the dissolved and suspended particulate phases (Fig. 8). For comparison with chondrite-normalized profiles of Fig. 8, North American Shale Composite (NASC) normalized REE patterns are shown in Fig. S.2 of the Supplementary Information.

The REE patterns in the dissolved phase (Fig. 8a) are characterized by flat to concave profiles with prominent negative Ce and Eu anomalies in some samples. The Ce anomalies are best explained by the oxidative precipitation of Ce(III) as insoluble Ce(IV): Plots of anomaly magnitude ($\log[Ce/Ce^*] = \log[2\ Ce_{CN}/(La_{CN} + Pr_{CN})]$) versus redox indicators show increasing magnitude with oxidizing conditions (Fig. S.3, Supplementary Information). The Eu anomalies, on the other hand, likely reflect the original REE composition of host rocks.

The fractionation patterns of REE in the dissolved phase are determined, in part, by complexation of REE with inorganic (Wood, 1990; Millero, 1992) or natural organic ligands (Tang and Johannesson, 2003; and references therein). For the circumneutral conditions observed here, carbonate ions (Smedley, 1991; Johannesson et al., 1996, 1999; 2000) represent the most likely inorganic agents whereas dissolved fulvic and humic acids are the most likely organic ligands (Tang and Johannesson, 2003; Rönnback et al., 2008; Pourret et al., 2010). The correlations shown in Fig. 9a and c suggest that stronger carbonate complexes are formed with heavy REE (HREE) than with light REE (LREE), which is consistent with previous experimental and field studies (Cantrell and Byrne, 1987; Smedley, 1991; Johannesson et al., 1999; Tang and Johannesson, 2005). The correlations shown in Fig. 9b and d, on the other hand, suggest that DOC may be a stronger complexation agent for dissolved LREE which is consistent with the speciation modeling results of Tang and Johannesson (2005).

The REE fractionation patterns in the suspended particulate phase (Fig. 8b) are characterized by a general decrease in enrichment from La to Gd and fairly flat profiles from Tb to Lu. Cerium anomalies are more muted than in the dissolved phase whereas Eu anomalies remain conspicuous. These patterns are determined, in part, by adsorption of REE on suspended particulates such as oxyhydroxides of Fe and Mn (Sholkovitz et al., 1994; De Carlo et al., 1998; Quinn et al., 2006; Leybourne and Johannesson, 2008). Particulate concentrations of representative LREE (La) and HREE (Dy) exhibit correlations with particulate concentrations of Al, Fe and

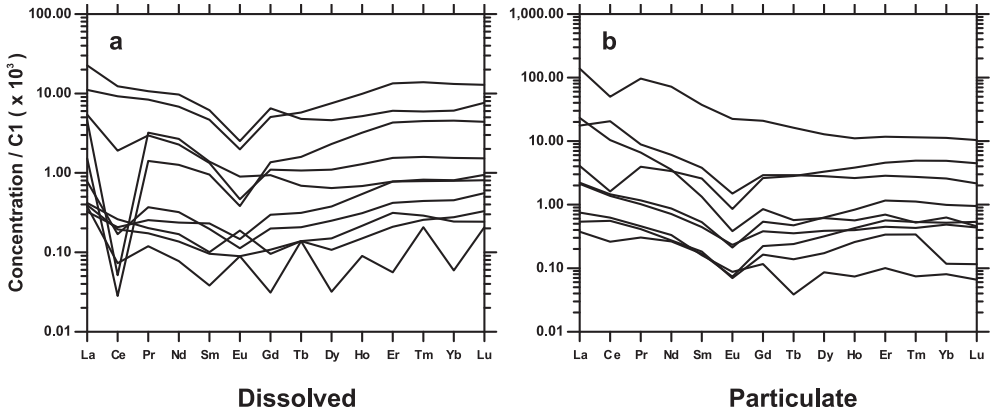

Fig. 8. Chondrite-normalized REE fractionation patterns for representative groundwaters from each of the 10 mineral deposits: (a) dissolved concentrations; (b) suspended particulate concentrations. C1-chondrite REE abundances are from Anders and Grevesse (1989).

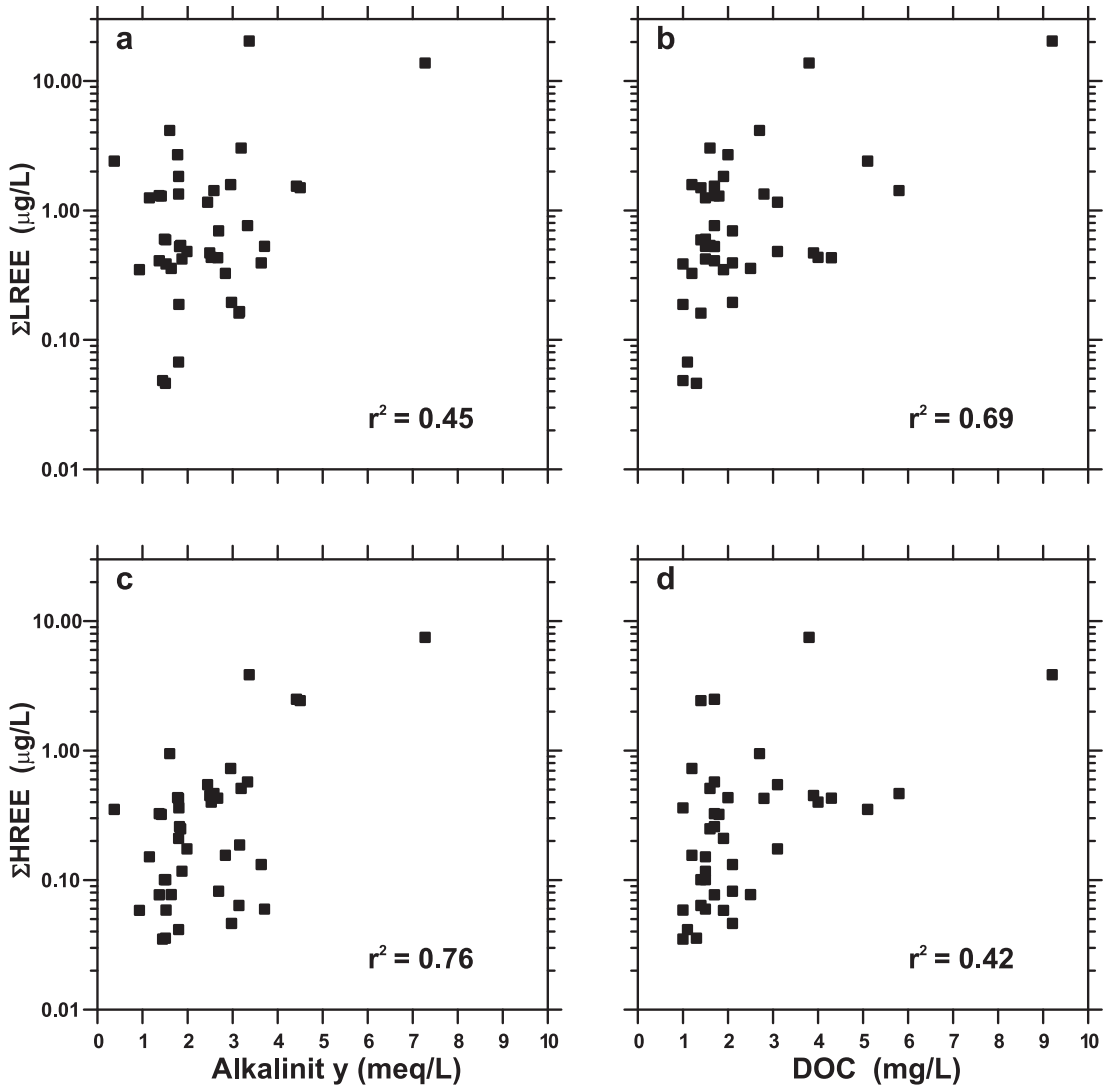

Fig. 9. Empirical evidence for REE complexation with carbonate and dissolved organic ligands: (a) Sum of LREE versus alkalinity; (b) Sum of LREE versus DOC; (c) Sum of HREE versus alkalinity; (d) Sum of HREE versus DOC.

Mn (Fig. S.4, Supplementary Information). However, correlations between REE and Mn are strongest, suggesting preferential sorption to particulate Mn. Chondrite-normalized concentrations of particulate LREE (La, Nd, Gd) show decreasing levels of sorption to Mn with increasing atomic number (Fig. 10a). Normalized concentrations of particulate HREE (Dy, Er, Yb), on the other hand, exhibit similar levels of sorption to Mn regardless of atomic number (Fig. 10b). These results are consistent with previous studies in which preferential adsorption of LREE compared to HREE was observed in the presence of strong ligands such as carbonate species (Smedley, 1991; Koeppenkastrop and De Carlo, 1992; Tang and Johannesson, 2005; Willis and Johannesson, 2011). Corresponding plots for NASC-normalized REE concentrations are provided in Fig. S.5 (Supplementary Information).

4.4. Mass balance modeling

The results of the previous sections illustrate some of the key factors that control the composition of individual trace elements in mine waters from granitic pegmatite U–Th–REE deposits. They can be enumerated as follows (after Langmuir, 1978):

1. The overall trace element abundance within the host mineral deposit.
2. The leachability of trace-element-bearing minerals.
3. The pH and p*e* of the groundwater.
4. The concentration of species that can form soluble complexes with trace elements or insoluble precipitates.
5. The concentration of highly sorptive species which can remove trace elements from solution.

Inverse modeling (Alpers and Nordstrom, 1999) provides a way of understanding U, Th, and REE mobilization through the interaction of these factors in the overarching context of mineral deposit weathering reactions. This section presents a comparative analysis of inverse modeling results for drainage chemistry from five different mine adits representing a range of geoenvironmental settings (Table 3).

Inverse modeling involves the simultaneous solution of mass balance equations for groundwater constituents:

Initial water composition + reactants
= Final water composition + products

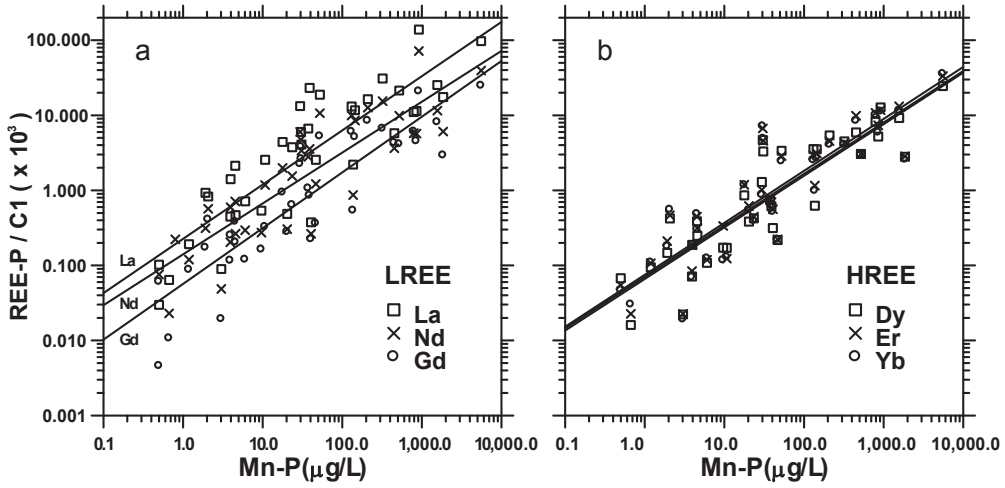

Fig. 10. Chondrite-normalized REE concentrations in the particulate phase versus particulate Mn concentration: (a) Light REE; (b) Heavy REE. Straight lines represent least-squares linear regression fits to data.

Table 3
Water chemistry analyses for samples used in inverse modeling: the initial water composition represents precipitation-weighted average concentrations in precipitation measured at Sprucedale, Ontario, during 2011 (Environment Canada, 2014b). Trace element concentrations in precipitation are assumed nil. Total (T) concentrations are used for trace elements in order not to underestimate reaction coefficients.

	Croft	Amalgamated rare earth #1	Amalgamated rare earth #2	Halo lake zone	Halo NW zone	Sprucedale precipitation
Temp (°C)	8.2	9.3	8.8	8.5	8.3	8.2
pH	7.66	7.77	7.49	7.46	8.05	4.8
pe	2.4	1.7	1.4	2.6	0.3	4.0
DOC (mg/L)	2.8	2.1	3.9	3.1	5.8	0.0
K (mg/L)	1.34	2.05	2.43	1.82	1.72	0.02
Na (mg/L)	2.84	2.06	4.38	2.17	2.03	0.04
Ca (mg/L)	41.84	66.32	39.43	44.41	51.03	0.14
Mg (mg/L)	3.31	3.35	6.87	5.41	6.17	0.02
Fe (μg/L)	11.40	24.00	347.00	32.00	90.00	0.00
Mn (μg/L)	1.46	31.00	386.00	6.00	25.00	0.00
Al (μg/L)	13.80	2.80	2.40	4.20	7.6	0.00
Ba (μg/L)	50.01	8.00	82.00	27.00	14.00	0.00
Pb (μg/L)	4.13	0.08	0.47	0.06	0.05	0.00
Cl (mg/L)	0.42	0.44	0.44	0.37	0.33	0.07
F (mg/L)	0.18	0.11	0.50	0.24	0.29	0.00
SO_4 (mg/L)	32.75	36.61	12.20	36.67	28.04	0.96
HCO_3 (mg/L)	109.86	181.68	152.05	121.20	157.78	0.00
SiO_2 (mg/L)	9.00	8.98	11.17	12.51	17.06	0.00
Ce–T (μg/L)	0.29	6.28	2.73	0.18	0.67	0.00
La–T (μg/L)	0.46	5.53	1.43	0.27	0.49	0.00
Mo (μg/L)	45.27	1.81	1.31	30.39	8.94	0.00
Nd–T (μg/L)	0.41	1.65	1.76	0.23	0.51	0.00
Th–T (μg/L)	0.09	11.56	2.05	n.d.	n.d.	0.00
U–T (μg/L)	596.64	401.65	298.75	248.30	44.46	0.00

Here, the initial water composition is that of precipitation measured at a site 100 km west of the study area in similar gneissic upland terrain (Sprucedale, Table 3). The final water composition is that of adit drainage (Table 3). The reactants and products are mineral or gaseous phases of known stoichiometry that dissolve or precipitate. Solution of the mass balance equations yields the moles of reactants or products per kg/H_2O that are required in order to account for the change in constituent concentrations between infiltrating precipitation and adit discharge.

The choice of mineral phases considered for inverse modeling is based initially on geological and mineralogical descriptions of the deposits (Satterly, 1957; Gordon et al., 1981; Sabina, 1986; Goad, 1990). However, the choice of any given mineral as a reactant or product is constrained by thermodynamic plausibility as characterized by the mineral's saturation index. Here, for example, either biotite or perthite (K-feldspar) could be considered as possible reactants yielding K. However, drainage waters are saturated with respect to K-feldspar and under-saturated with respect to biotite suggesting that biotite is a more likely source of dissolved K. In other cases, thermodynamic considerations are not sufficient to determine the most appropriate reactant minerals and it must be recognized that results of inverse modeling are inherently non-unique. Here, a ferromagnesian silicate reactant mineral is required in order to account for the Mg content of drainage waters. Both pyroxene and amphibole are present, in varying proportions, at all the deposits, and drainage waters are under-saturated with respect to both minerals. Equally good inverse models can be obtained using either mineral as a main source of Mg. However, only the results for amphibole are presented here. Similarly, both uraninite and uranothorite represent plausible mineral reactants containing U and Th. However, only the results for uranothorite are shown here because it is the dominant U–Th mineral in all but one

of the deposits considered.

Compositions for mineral reactants are shown in Table 4. These compositions were obtained from the literature or were determined by electron microprobe analysis as part of this study. For other minerals not listed, ideal compositions were assumed. The formulae for amphibole (hastingsite or magnesiohastingsite) and for biotite (Lentz, 1992) show that cation compositions are relatively stable whereas F and Cl compositions vary considerably. Therefore, in order to facilitate comparative inverse modeling using the same set of reactant and product compositions for each deposit, F and Cl were not included in mass balance calculations. The major cation composition of allanite in the Bancroft area is also quite stable (Peterson and MacFarlane, 1993) although the relative proportion of LREE (La, Ce, Nd) is more variable. Here, a representative cation composition is assumed (based on a sample from the Bicroft mine) and the relative proportion of La, Ce and Nd is adjusted for each deposit (Table 4). No attempt was made to include less abundant HREE in the mass balance calculations. Although drainage waters are under-saturated with respect to ideal birnessite, this mineral is used as a proxy for the unknown precipitating Mn phase. Removal of Th and radiogenic Pb from solution was represented in PHREEQC using a cation exchange reaction as suggested in Alpers and Nordstrom (1999).

Inverse modeling results for adit drainage from the five mineral deposits are summarized in Table 5. All five deposits are associated with granitic pegmatite intrusions although metasomatic reactions with different host rocks have imparted local variations to the typical mineralogy. Nonetheless, weathering of a relatively small number of common rock-forming and accessory minerals can readily account for the major and trace element chemistry of all five drainages.

Calcite weathering, with consumption of atmospheric CO_2, is the most significant water-rock reaction in molar terms (Table 5). Calcite is associated with pegmatite dykes at all deposits and is also found in marble host rocks of the Amalgamated Rare Earth No.1 (ARE1) and Halo North West Zone (HNWZ) adits. Drainage waters are in approximate equilibrium with calcite ($-0.47 < SI < 0.27$). In terms of factors influencing trace element mobility, calcite weathering buffers drainage pH and supplies Ca and carbonate complexing agents that increase the mobility of U (Fig. 5) and possibly HREE (Fig. 9c).

Bulk host rock composition is reflected in the reaction coefficients for plagioclase, biotite and amphibole. The more mafic nature of host rocks from the Amalgamated Rare Earth No.2 (ARE2) and Halo deposits is apparent from these coefficients. Weathering of these silicates contributes Si and Al to mine drainage which is saturated with respect to chalcedony (SiO_2) and $Al(OH)_3$. Weathering of biotite and amphibole (and/or pyroxene) contributes Fe, Mg and Mn. These waters are saturated with respect to Fe and Mn oxyhydroxides and precipitate amorphous $Fe(OH)_3$ and birnessite (Table 5). Iron precipitates likely sorb Th (Fig. 7) whereas Mn precipitates sorb REE (Fig. 10).

Pyrite is the main sulfide mineral in these deposits. Although its in-situ abundance is low, it is readily weathered as reflected by the relatively high reaction coefficients shown in Table 5. Pyrite oxidation, with consumption of O_2, contributes acidity, sulfate and Fe to mine drainage. The acidity is neutralized mainly by calcite dissolution and the Fe largely precipitates as amorphous $Fe(OH)_3$.

Allanite is notably abundant at the ARE1 and ARE2 deposits but less so at the other deposits (Satterly, 1957; Sabina, 1986). The relative abundance of allanite in the five deposits is reflected by the relative magnitude of the reaction coefficients in Table 5. However, the low absolute values of these reaction coefficients are indicative of the low in-situ allanite content of the deposits. Nonetheless, allanite weathering releases small amounts of LREE to mine drainage which appear to sorb preferentially to Mn precipitates (Fig. 10).

Since uranothorite is the only U-bearing mineral considered in mass balance modeling, the reaction coefficients for uranothorite (Table 5) directly mirror U concentrations in mine drainage (Table 3). Interestingly, these reactions coefficients appear uncorrelated with the U grades of the deposits (Table 5). The mineralogy of the dominant U-bearing phase in each deposit (Satterly, 1957; Gordon et al., 1981) may offer some explanation. In the Croft and ARE1 adits, uranothorite is the only U-bearing ore mineral. In the ARE2 and Halo-Lake Zone adits, uranothorite is the main ore mineral although some uraninite is present. In the HNWZ adit, uraninite is the main ore mineral and uranothorite is uncommon, which is unusual for the Bancroft mining camp (Satterly, 1957). Thus, U concentrations in mine drainage and reaction coefficients may reflect the uranothorite content of the deposits rather than their overall U grade. With its usually metamict and hydrated structure (Robinson and Abbey, 1957), uranothorite may be more easily weathered than uraninite. The actual U release mechanisms are likely more complicated since U occurs not only in primary uraninite and uranothorite grains but also in chemically-complex fracture fillings re-precipitated from aqueous solutions (Rimsaite, 1982). Uranium in fractures is more accessible to leaching and may represent the source of most of the load discharged from the adits. The mobility of U, therefore, depends not only on the mineralogy of primary U-bearing minerals but also on their history of in-situ alteration and redistribution (Krall et al., 2015).

Based on the stoichiometries of uranothorite or uraninite (Table 4), the release of U at the levels observed must have been

Table 4
Composition of selected mineral reactants in samples from Bancroft area granitic pegmatite U–Th–REE deposits, as indicated. Compositions are from the literature or from microprobe analyses conducted as part of this study.

Mineral	Formula	Reference
Perthite	$K_{0.77}Na_{0.22}Ca_{0.01}Al_{1.01}Si_{2.99}O_8$	Goad (1990); Croft
Plagioclase	$Na_{0.75}Ca_{0.25}Al_{1.25}Si_{2.75}O_8$	Burton (1984); Croft
Pyroxene	$Ca_{0.95}Na_{0.05}Mg_{0.62}Fe_{0.34}Mn_{0.02}Al_{0.11}Si_{1.94}O_6$	This study; Halo
Amphibole	$Na_{0.58}K_{0.33}Ca_{1.79}Mg_{2.07}Fe_{2.65}Mn_{0.12}Al_{1.71}Si_{6.55}O_{22}(OH)_{1.4}F_{0.45}Cl_{0.15}$	This study; Croft
Amphibole	$Na_{0.42}K_{0.49}Ca_{1.94}Mg_{2.57}Fe_{2}Mn_{0.04}Al_{2.31}Si_{6.12}O_{22}(OH)_{1.49}F_{0.4}Cl_{0.11}$	This study; Halo
Amphibole	$Na_{0.6}K_{0.37}Ca_{1.85}Mg_{1.87}Fe_{2.67}Mn_{0.05}Al_{2.15}Si_{6.33}O_{22}(OH)_{1.77}F_{0.16}Cl_{0.07}$	This study; ARE2
Amphibole	$Na_{0.58}K_{0.33}Ca_{1.79}Mg_{2.07}Fe_{2.65}Mn_{0.12}Al_{1.71}Si_{6.55}O_{22}(OH)_2$	Used in modeling
Biotite	$K_{0.95}Mg_{1.52}Fe_{1.05}Mn_{0.02}Al_{1.25}Si_{3.03}O_{10}(OH)_{1.32}F_{0.6}Cl_{0.08}$	This study; Croft
Biotite	$K_{0.99}Mg_{2.14}Fe_{0.7}Mn_{0.01}Al_{0.97}Si_{3.1}O_{10}(OH)_{0.82}F_{1.15}Cl_{0.03}$	Lentz (1992); Kenmac-Chibou.
Biotite	$K_{0.95}Mg_{1.52}Fe_{1.05}Mn_{0.02}Al_{1.25}Si_{3.03}O_{10}(OH)_2$	Used in modeling
Uraninite	$U_{0.74}Th_{0.09}Pb_{0.17}O_{1.83}$	Robinson and Sabina (1955); Bicroft
Uranothorite	$Th_{0.74}U_{0.15}Fe_{0.12}Ca_{0.19}Pb_{0.05}Si_{1.1}O_4$	Robinson and Abbey (1957); Bicroft
Allanite	$Ca_{1.16}La_{0.24}Ce_{0.39}Nd_{0.13}Fe_{1.23}Al_{1.71}Si_{3.03}O_{12}(OH)$	Peterson and MacFarlane (1993); Bicroft
Allanite	$Ca_{1.16}$ (La, Ce, Nd) $_{0.76}Fe_{1.23}Al_{1.71}Si_{3.03}O_{12}(OH)$	Used in modeling

Table 5
Reaction coefficients (moles/kg H_2O) obtained for inverse modeling of adit discharge chemistry in five granitic pegmatite U–Th–REE deposits. They are positive for reactants and negative for products. The estimated grade and main U-bearing mineral for each deposit are listed at the foot of the table.

Reactant/product	Croft	Amalgamated rare earth #1	Amalgamated rare earth #2	Halo Lake zone	Halo NW zone
Calcite	8.93 E-04	1.57 E-03	6.91 E-04	8.91 E-04	1.04 E-04
Plagioclase	1.23 E-04	9.02 E-05	1.60 E-04	4.93 E-04	2.35 E-05
Biotite	1.93 E-05	4.25 E-05	2.36 E-05	1.51 E-05	4.47 E-06
Amphibole	5.12 E-05	3.49 E-05	1.19 E-04	9.60 E-05	1.19 E-04
Pyrite	1.63 E-04	1.84 E-04	5.64 E-05	1.84 E-04	1.39 E-04
Molybdenite	4.72 E-07	1.89 E-08	1.36 E-08	3.17 E-07	9.32 E-08
Barite	3.65 E-07	5.83 E-08	5.97 E-07	1.97 E-07	1.02 E-07
Allanite	1.08 E-08	1.27 E-07	5.56 E-08	6.46 E-09	1.54 E-08
Uranothorite	1.67 E-05	1.12 E-05	8.37 E-06	6.96 E-06	1.25 E-06
O_2 (g)	6.50 E-04	7.22 E-04	2.84 E-04	7.52 E-04	5.93 E-04
CO_2 (g)	1.00 E-03	1.52 E-03	2.01 E-03	1.28 E-03	1.58 E-03
Chalcedony	−6.00 E-04	−4.69 E-04	−1.11 E-03	−6.09 E-04	−5.74 E-04
$Al(OH)_3$(a)	−2.65 E-04	−2.26 E-04	−4.32 E-04	−2.45 E-04	−2.38 E-04
$Fe(OH)_3$(a)	−3.21 E-04	−3.22 E-04	−3.91 E-04	−4.54 E-04	−4.57 E-04
Birnessite(a)	−6.50 E-06	−4.48 E-06	−7.69 E-06	−1.17 E-05	−1.39 E-05
X_4-Th	−9.02 E-06	−6.03 E-06	−4.51 E-05	−3.76 E-06	−6.73 E-07
Grade (% U_3O_8)[a]	0.061	0.110	0.095	0.112	0.112
Main ore mineral[b]	Uranothorite	Uranothorite	Uranothorite	Uranothorite	Uraninite

[a] Grade estimates are from Gordon et al. (1981) except for the Croft mine (Burton, 1984).
[b] Main ore minerals are from Gordon et al. (1981).

accompanied by a corresponding release of Th, far in excess of what is measured in groundwaters in either the dissolved or particulate phases. The Th-sink (X_4-Th) reaction coefficients in Table 5 reflect this near total immobilization of Th close to its source.

5. Summary and conclusions

Small, low-grade, granitic pegmatite hosted U–Th–REE deposits are found throughout the Grenville geological province of eastern Canada. They are particularly numerous in the Bancroft area of Ontario where four deposits were brought into production and several others reached advanced stages of pre-mining development. Investigations into groundwater quality at 10 historical mining properties focused on the mobility of trace elements that may pose health risks.

Uranium, almost entirely in the dissolved phase (<0.45 μm), was observed at concentrations ranging of up to 2579 μg/L. The Canadian regulatory limit for U in drinking water (0.02 mg/L) was exceeded in 70% of samples. Uraninite and uranothorite are the main U-bearing minerals and were present in varying proportions in all the deposits sampled. The highest U concentrations were found to occur in mine waters associated with deposits where uranothorite is the dominant U host. Because of its metamict structure and non-ideal composition, uranothorite may weather more readily than uraninite. Speciation modeling results indicate that U(VI) released by the oxidation and dissolution of uraninite or uranothorite occurs almost entirely as stable uranyl-Ca–carbonate complexes. The Ca and carbonate complexing agents are provided by the dissolution of calcite, a ubiquitous accessory mineral. Recent literature suggest that these complexes may inhibit processes that immobilize U(VI) such as adsorption to Fe oxyhydroxides and bioreduction to U(IV). The activities of U decay products, ^{226}Ra and ^{210}Pb, are well correlated although they are only weakly correlated with U concentrations. Generally, regulatory limits for ^{226}Ra and ^{210}Pb were exceeded only when limits for U were exceeded as well. The data suggest that U and ^{210}Pb are relatively more mobile under oxic conditions whereas ^{226}Ra is relatively more mobile under reducing conditions.

Thorium is released concomitantly with U during the dissolution of uranothorite or Th-bearing uraninite. However, concentrations of Th in both filtered and unfiltered samples are extremely low (<11 μg/L). Mass balance calculations indicate that almost all dissolved Th must be immobilized close to its source. Most of the remaining Th appears to be sorbed to particulate Fe oxyhydroxides derived mainly from the dissolution of ferromagnesian silicate minerals.

Total light REE concentrations range between 0.1 and 117 μg/L while heavy REE concentrations vary between 0.05 and 21 μg/L. The main source of LREE is allanite. Although not abundant, it may dissolve readily because of its metamict structure. The sources of HREE are widely dispersed among the exotic minerals associated with Bancroft area granitic pegmatite deposits. Various processes such as complexation and adsorption, as well as local redox conditions, have acted on original host-rock compositions and have shaped distinct groundwater REE fractionation patterns in the dissolved and suspended particulate phases. The REE fractionation pattern in the dissolved phase is flat to slightly concave with prominent negative Ce anomalies in more oxidizing waters. The data suggest that LREE may tend to form soluble complexes with organic ligands whereas HREE may have more affinity for carbonate ions. The REE fractionation pattern in the suspended particulate phase shows decreasing enrichment with atomic number across the LREE range (La–Gd) and a flat profile across the HREE range (Tb–Lu). Adsorption is greatest for La and decreases with atomic number across the LREE range. Sorption of HREE appears independent of atomic number. Manganese precipitates of unknown structure appear to be the favored species for REE adsorption.

The results of this study provide a benchmark for assessing environmental and health risks from trace elements in mine drainage from granitic pegmatite U–Th–REE deposits yet to be developed. Based on their very low mobility in groundwater, Th and REE are unlikely to represent an environmental concern. Uranium, on the other hand, exhibits very high mobility in shallow, oxic, groundwaters associated with some deposits. Because of this mobility and its toxicity, drainage from some mine workings may require U mitigation measures in order to avoid environmental impacts to downstream surface waters.

Acknowledgments

This project was supported by the Environmental Geosciences Program of the Earth Sciences Sector of Natural Resources Canada.

Judy Vaive and Pierre Pelchat of the Geological Survey of Canada Inorganic Geochemical Research Laboratory performed the water chemistry analyses. Michael Parsons and two anonymous reviewers provided helpful comments on earlier versions of this paper. Data presented in this paper are publically available in Desbarats and Percival (2016). Earth Sciences Sector contribution 20150266.

Appendix A. Supplementary data

Supplementary data related to this article can be found at http://dx.doi.org/10.1016/j.apgeochem.2016.02.010.

References

Alexander, R.L., 1986. Geology of Madawaska Mines Ltd., Bancroft, Ontario. In: Evans, E.L. (Ed.), Uranium Deposits in Canada, Special vol. 33. Can. Inst. Mining Metall, pp. 62–69.

Alpers, C.N., Nordstrom, D.K., 1999. Geochemical modeling of water-rock interactions in mining environments. In: Plumlee, G.S., Logsdon, M.J. (Eds.), The Environmental Geochemistry of Mineral Deposits Part A: Processes, Techniques and Health Issues, Soc. Econ. Geol. Reviews in Economic Geology, vol. 6A, pp. 289–323.

Anders, E., Grevesse, N., 1989. Abundances of the elements: meteoritic and solar. Geochim. Cosmochim. Acta. 53, 197–214.

Armstrong, J.T., 1988. Quantitative analysis of silicates and oxide minerals: comparison of Monte-Carlo, ZAF and Phi-Rho-Z procedures. In: Newbury, D.E. (Ed.), Microbeam Analysis. San Francisco Press, San Francisco, pp. 239–246.

Asikainen, M., 1981. State of disequilibrium between ^{238}U, ^{234}U, ^{226}Ra and ^{222}Rn in groundwater from bedrock. Geochim. Cosmochim. Acta 45, 201–206.

ATSDR, 1990. Toxicological Profile for Thorium. Agency for Toxic Substances and Disease Registry. U.S. Public Health Service, Atlanta, GA, p. 174.

Ayotte, J.D., Flanagan, S.M., Morrow, W.S., 2007. Occurrence of Uranium and ^{222}Radon in Glacial and Bedrock Aquifers in the Northern United States, 1993-2003. U.S. Geol. Surv. Sci. Investigations Rep. 2007-5037, Reston, Va, p. 84.

Ball, J.W., Nordstrom, D.K., 1991. User's Manual for WATEQ4F with Revised Thermodynamic Database and Test Cases for Calculating Speciation of Major, Trace, and Redox Elements in Natural Waters. US Geol. Surv. Open-File Report 91–183, Reston, VA.

Banks, D., Røyset, O., Strand, T., Skarphagen, H., 1995. Radioelement (U, Th, Rn) concentrations in Norwegian bedrock groundwater. Env. Geol. 25 (3), 165–180.

Bernhard, G., Geipel, G., Brendler, V., Nitsche, H., 1996. Speciation of uranium in seepage waters of a mine tailing pile studied by time-resolved laser-induced fluorescence spectroscopy (TRLFS). Radiochim. Acta 74, 87–91.

Brooks, S.C., Fredrickson, J.K., Carroll, S.L., Kennedy, D.W., Zachara, J.M., Plymale, A.E., Kelly, S.D., Kemner, K.M., Fendorf, S., 2003. Inhibition of bacterial U(VI) reduction by calcium. Environ. Sci. Technol. 37, 1850–1858. http://dx.doi.org/10.1012/es0210042.

Burton, D.M., 1984. The Geology of the CAM Uranium Deposit, Cardiff Township, Ontario, Canada (M.Sc. thesis). Dept. of Geology, University of New Brunswick, Fredericton, NB, p. 206.

Campbell, K.M., Gallegos, T.J., Landa, E.R., 2015. Biogeochemical aspects of uranium mineralization, mining, milling and remediation. Appl. Geochem. 57, 206–235. http://dx.doi.org/10.1016/j.apgeochem.2014.07.022.

Cantrell, K.J., Byrne, R.H., 1987. Rare earth element complexation by carbonate and oxalate ions. Geochim. Cosmochim. Acta 51, 597–605.

Chamberlain, J.A., 1964. Hydrogeochemistry of uranium in the Bancroft-Haliburton Region, Ontario. Geol. Surv. Can. Bull. 118, 19. Ottawa, ON.

Cothern, R.C., Rebers, P.A. (Eds.), 1990. Radon, Radium and Uranium in Drinking Water. Lewis Publishers, Chelsea, MI, p. 286.

De Carlo, E.H., Wen, X., Irving, M., 1998. The influence of redox reactions on the uptake of dissolved Ce by suspended Fe and Mn oxide particles. Aquat. Chem. 3, 357–389.

Degueldre, C., Kline, A., 2007. Study of thorium association and surface precipitation on colloids. Earth Plan. Sci. Lett. 264, 104–113. http://dx.doi.org/10.1016/j.epsl.2007.09.012.

De Pablo, J., Casas, I., Giménez, J., Molera, M., Rovira, M., Duro, L., Bruno, J., 1999. The oxidative dissolution mechanism of uranium dioxide. I. The effect of temperature in hydrogen carbonate medium. Geochim. Cosmochim. Acta 63, 3097–3103.

Desbarats, A.J., Percival, J.B., 2016. Groundwater Chemistry of Uranium-thorium-rare Earth Element Deposits, Bancroft Area. Ontario. Geol. Surv. Canada, Open File Rep. 7992, Ottawa, ON.

Dia, A., Gruau, G., Olivié-Lauquet, G., Riou, C., Molénat, J., Curmi, P., 2000. The distribution of rare earth elements in groundwaters: assessing the role of source-rock composition, redox changes and colloidal particles. Geochim. Cosmochim. Acta 64, 4131–4151.

Dong, W., Brooks, S.C., 2006. Determination of the formation constants of ternary complexes of uranyl and carbonate with alkaline earth metals (Mg^{2+}, Ca^{2+}, Sr^{2+}, and Ba^{2+}) using anion exchange method. Environ. Sci. Technol. 40, 4689–4695. http://dx.doi.org/10.1021/es0606327.

Dong, W., Brooks, S.C., 2008. Formation of aqueous $MgUO_2(CO_3)_3^{2-}$ complex and uranium anion exchange mechanism onto an exchange resin. Environ. Sci. Technol. 42, 1979–1983. http://dx.doi.org/10.1021/es0711563.

Easton, R.M., 1992. The Grenville Province and the Proterozoic history of Central and southern Ontario. In: Thurston, P.C., Williams, H.R., Sutcliffe, R.H., Stott, G.M. (Eds.), Geology of Ontario, Ontario Geol. Surv, Spec. vol. 4 chap. 19, pp. 715–904, Toronto, ON.

Easton, R.M., Fyon, J.A., 1992. Metallogeny of the Grenville Province. In: Thurston, P.C., Williams, H.R., Sutcliffe, R.H., Stott, G.M. (Eds.), Geology of Ontario, Ontario Geol. Surv., Spec. vol. 4 chap. 24, pp. 1217–1252, Toronto, ON.

Environment Canada, 2014a. Canadian Climate Normals 1981-2010 Station Data. Downloaded from. http://climate.weather.gc.ca/climate_normals/.

Environment Canada, 2014b. The Canadian National Atmospheric Chemistry (NAtChem) Database and Analysis System. Downloaded from. http://www.ec.gc.ca/natchem/.

EPA, 2012. Rare Earth Elements: a Review of Production, Processing, Recycling, and Associated Environmental Issues. U.S. Environ. Protect. Agency, Office of Research and Development, Cincinnati, OH. Rep. EPA/600/R-12/572.

Ercit, T.S., 2002. The mess that is "allanite". Can. Mineral. 40, 1411–1419.

Focazio, M.J., Szabo, Z., Kraemer, T.F., Mullin, A.H., Barringer, T.H., dePaul, V.T., 2001. Occurrence of Selected Radionuclides in Ground Water Used for Drinking Water in the United States: a Reconnaissance Survey, 1998. U.S. Geol. Surv. Water Resour. Investigations. Rep. 00-4723, Reston, VA, p. 40.

Fox, P.M., Davis, J.A., Zachara, J.M., 2006. The effect of calcium on aqueous uranium(VI) speciation and adsorption to ferrihydrite and quartz. Geochim. Cosmochim. Acta 70, 1379–1387. http://dx.doi.org/10.106/j.gca.2005.11.027.

Gannon, J.P., Burbey, T.J., Bodnar, R.J., Aylor, J., 2012. Geophysical and geochemical characterization of the groundwater system and the role of the Chatham Fault in groundwater movement at the Coles Hill uranium deposit, Virginia, U.S.A. Hydrogeol. J. 20, 45–60. http://dx.doi.org/10.1007/s10040-011-0798-y.

Gascoyne, M., 1989. High levels of uranium and radium in groundwaters at Canada's Underground Research Laboratory, Lac du Bonnet, Manitoba, Canada. Appl. Geochem. 4, 577–591.

Goad, B.E., 1990. Granitic pegmatites of the Bancroft area, southeastern Ontario. Ontario Geol. Surv., Open File Rep. 5717, Toronto, ON, p. 459.

Gomez, P., Garralon, A., Biul, B., Turrero, Ma J., Sanchez, L., de la Cruz, B., 2006. Modeling of geochemical processes related to uranium mobilization in the groundwater of a uranium mine. Sci. Tot. Env. 366, 295–309. http://dx.doi.org/10.1016/j.scitotenv.2005.06.024.

Gordon, J.B., Rybak, U.C., Robertson, J.A., 1981. Uranium and thorium deposits of southern Ontario. Ontario Geol. Surv., Open File Rep. 5311, Toronto, ON, p. 665.

Grandstaff, D.E., 1976. A kinetic study of the dissolution of uraninite. Econ. Geol. 71, 1493–1506.

Griffith, J.W., 1986. Uranium deposits of the Bancroft area, Ontario. In: Evans, E.L. (Ed.), Uranium Deposits in Canada, Special vol. 33. Can. Inst. Mining Metall., pp. 57–61

Health Canada, 2001. Guidelines for Canadian Drinking Water Quality – Technical Document: Uranium, Water and Air Quality Bureau, Healthy Environments and Consumer Safety Branch. Health Canada, Ottawa, ON, p. 10.

Health Canada, 2010. Guidelines for Canadian Drinking Water Quality – Technical Document: Radiological Parameters, Water and Air Quality Bureau, Healthy Environments and Consumer Safety Branch. Health Canada, Ottawa, ON, p. 46.

Health Canada, 2014. Guidelines for Canadian Drinking Water Quality – Summary Table. Water and Air Quality Bureau, Healthy Environments and Consumer Safety Branch. Health Canada, Ottawa, ON, p. 25.

Hem, J.D., Cropper, W.H., 1959. Survey of Ferrous-ferric Chemical Equilibria and Redox Potentials. U.S. Geol. Surv. Water-Supply Paper 1459-A, Washington, DC.

Hewitt, D.F., 1967. Uranium and Thorium Deposits of Southern Ontario. Ontario Dept. Mines, Mineral Res. Circ. No. 4, Toronto, ON, p. 76.

Janezcek, J., Ewing, R.C., 1992. Structural formula of uraninite. J. Nucl. Mater. 190, 128–132.

Jerden Jr., J.L., Sinha, A.K., 2003. Phosphate based immobilization of uranium in an oxidizing bedrock aquifer. Appl. Geochem. 18, 823–843.

Johannesson, K.H., Stetzenbach, K.J., Hodge, V.F., Lyons, W.B., 1996. Rare earth element complexation behavior in circumneutral pH groundwaters: assessing the role of carbonate and phosphate ions. Earth Plan. Sci. Lett. 139, 305–319.

Johannesson, K.H., Farnham, I.M., Guo, C., Stetzenbach, K.J., 1999. Rare earth element fractionation and concentration variations along a groundwater flow path within a shallow, basin-fill aquifer, southern Nevada, USA. Geochim. Cosmochim. Acta 63, 2697–2708.

Johannesson, K.H., Zhou, X., Guo, C., Stetzenbach, K.J., Hodge, V.F., 2000. Origin of rare earth element signatures in groundwaters of circumneutral pH from southern Nevada and eastern California, USA. Chem. Geol. 164, 239–257.

Kelly, S.D., Kemner, K.M., Brooks, S.C., 2007. X-ray absorption spectroscopy identifies calcium-uranyl-carbonate complexes at environmental concentrations. Geochim. Cosmochim. Acta 71, 821–834. http://dx.doi.org/10.1016/j.gca.2006.10.013.

Koeppenkastrop, D., De Carlo, E.H., 1992. Sorption of rare-earth elements from seawater onto synthetic mineral particles: an experimental approach. Chem. Geol. 95, 251–263.

Krall, L., Sandström, B., Tullborg, E.-L., Evins, L.Z., 2015. Natural uranium in Forsmark, Sweden: the solid phase. Appl. Geochem. 59, 178–188. http://dx.doi.org/10.1016/j.apgeochem.2015.04.020.

Lahermo, P., Juntunen, R., 1991. Radiogenic elements in Finnish soils and

groundwaters. Appl. Geochem. 6, 169–183.
Langmuir, D., 1978. Uranium solution-mineral equilibria at low temperatures with applications to sedimentary ore deposits. Geochim. Cosmochim. Acta 42, 547–569.
Langmuir, D., Herman, J.S., 1980. The mobility of thorium in natural waters at low temperatures. Geochim. Cosmochim. Acta. 44, 1753–1766.
Lentz, D., 1991. Radioelement distribution in U, Th, Mo, and rare-earth-element pegmatites, skarns, and veins in a portion of the Grenville Province, Ontario and Quebec. Can. J. Earth Sci. 28, 1–12.
Lentz, D., 1992. Petrogenesis and geochemical composition of biotites in rare-element granitic pegmatites in the southwestern Grenville Province, Canada. Mineral. Petrol. 46, 239–256.
Lentz, D., 1996. U, Mo, and REE mineralization in late-tectonic granitic pegmatites, southwestern Grenville Province, Canada. Ore Geol. Rev. 11, 197–227.
Leybourne, M.I., Johannesson, K.H., 2008. Rare earth elements (REE) and yttrium in stream waters, stream sediments, and Fe-Mn oxyhydroxides: fractionation, speciation, and controls over REE+Y patterns in the surface environment. Geochim. Cosmochim. Acta 72, 5962–5983. http://dx.doi.org/10.1016/j.gca.2008.09.022.
Lumbers, S.B., Heaman, L.M., Vertolli, V.M., Wu, T.W., 1990. Nature and timing of Middle Proterozoic magmatism in the Central Metasedimentary Belt, Grenville Province, Ontario. In: Gower, C.F., Rivers, T., Ryan, B. (Eds.), Mid-Proterozoic Laurentia-Baltica, Geol. Assoc. Can., Spec. Pap. 38, pp. 243–276.
Millero, F.J., 1992. Stability constants for the formation of rare earth inorganic complexes as a function of ionic strength. Geochim. Cosmochim. Acta 56, 3123–3132.
Ontario Geological Survey, 1991. Bedrock Geology of Ontario, Southern Sheet. Ont. Geol. Surv.. Map 2544, scale 1:1,000,000.
Pagano, G., Guida, M., Tommasi, F., Oral, R., 2015. Health effects and toxicity mechanisms of rare earth elements – knowledge gaps and research prospects. Ecotox. Environ. Saf. 115, 40–48. http://dx.doi.org/10.1016/j.ecoenv.2015.01.030.
Parc, S., Nahon, D., Tardy, Y., Veillard, P., 1989. Estimated solubility products and fields of stability for cryptomelane, nsutite, birnessite, and lithiophorite based on natural lateritic weathering sequences. Am. Mineral. 74, 466–475.
Parkhurst, D.L., Appelo, C.A.J., 1999. User's Guide to PHREEQC (Version 2) – a Computer Program for Speciation, Batch Reaction, One-dimensional Transport, and Inverse Geochemical Calculations. U.S. Geol. Surv. Water-Resources Investigations Report 99–4259.
Peterson, R.C., MacFarlane, D.B., 1993. The rare-earth-element chemistry of allanite from the Grenville Province. Can. Mineral. 31, 159–166.
Plummer, L.N., Parkhurst, D.L., Thorstenson, D.C., 1983. Development of reaction models for ground-water systems. Geochim. Cosmochim. Acta. 47 (4), 665–686.
Pourret, O., Gruau, G., Dia, A., Davranche, M., Molénat, J., 2010. Colloidal control on the distribution of rare earth elements in shallow groundwaters. Aquat. Geochem. 16, 31–59. http://dx.doi.org/10.1007/s10498-009-9069-0.
Prat, O., Vercouter, T., Ansoborlo, E., Fichet, P., Perret, P., Kurttio, P., Salonen, L., 2009. Uranium speciation in drinking water from drilled wells in southern Finland and its potential links to health effects. Environ. Sci. Technol. 43, 3941–3946. http://dx.doi.org/10.1021/es803658e.
Price, J.R., Velbel, M.A., Patino, L.C., 2005. Allanite and epidote weathering at the Coweeta Hydrologic Laboratory, western North Carolina, U.S.A. Am. Mineral. 90, 101–114. http://dx.doi.org/10.2138/am.2005.1444.
Quinn, K.A., Byrne, R.H., Schijf, J., 2006. Sorption of yttrium and rare earth elements by amorphous ferric hydroxide: influence of solution complexation with carbonate. Geochim. Cosmochim. Acta 70, 4151–4165. http://dx.doi.org/10.1016/j.gca.2006.06.014.
Richardson, D.G., Birkett, T.C., 1996. Peralkaline rock-associated rare metals. In: Eckstrand, O.R., Sinclair, W.D., Thorpe, R.I. (Eds.), Geology of Canadian Mineral Deposit Types, Geology of Canada, vol. 8. Geol. Surv. Can., Ottawa, ON, pp. 523–540.
Rimsaite, J., 1982. Alteration of radioactive minerals in granite and related secondary uranium mineralizations. In: Amstutz, G.C., El Goresy, A., Frenzel, G., Kluth, C., Moh, G., Wauschkuhn, A., Zimmermann, R.A. (Eds.), Ore Genesis: the State of the Art. Springer-Verlag, Berlin, pp. 269–280.
Robinson, S.C., Sabina, A.P., 1955. Uraninite and thorianite from Ontario and Quebec. Am. Mineral. 40, 624–633.
Robinson, S.C., Abbey, S., 1957. Uranothorite from eastern Ontario. Can. Mineral. 6, 1–15.
Rogers, J.J., Ragland, P.C., Nishimori, R.K., Greenberg, J.K., Hauck, S.A., 1978. Varieties of granitic uranium deposits and favorable exploration areas in the Eastern United States. Econ. Geol. 73, 1539–1555.
Rönnback, P., Åström, M., Gustafsson, J.-P., 2008. Comparison of the behaviour of rare earth elements in surface waters, overburden groundwaters and bedrock groundwaters in two granitoidic settings, Eastern Sweden. Appl. Geochem. 23, 1862–1880. http://dx.doi.org/10.1016/j.apgeochem.2008.02.008.
Sabina, A.P., 1986. Rocks and minerals for the collector, Bancroft – Parry Sound area and Southern Ontario. Geol. Surv. Can. Misc. Rep. 39, 182 (Ottawa, ON).
Satterly, J., 1957. Radioactive Mineral Occurrences in the Bancroft Area. Ontario Dept. Mines, 65th Ann. Rep., Part 6, 1956, p. 176 (Toronto, ON).
Sholkovitz, E.R., Landing, W.M., Lewis, B.L., 1994. Ocean particle chemistry: the fractionation of rare earth elements between suspended particles and seawater. Geochim. Cosmochim. Acta 58, 1567–1579.
Smedley, P.L., 1991. The geochemistry of rare earth elements in groundwater from the Carnmenellis area, southwest England. Geochim. Cosmochim. Acta 55, 2767–2779.
Stewart, B.D., Mayes, M.A., Fendorf, S., 2010. Impact of uranyl-calcium-carbonato complexes on uranium(VI) adsorption to synthetic and natural sediments. Environ. Sci. Technol. 44, 928–934. http://dx.doi.org/10.1021/es902194x.
Strong, W.L., Zoltai, S.C., Ironside, G.R., 1989. Ecoclimatic Regions of Canada. In: Ecological Land Classification Series, vol. 23. Canadian Wildlife Service, Environment Canada, Ottawa, p. 122.
Szabo, Z., Zapecza, O.S., 1991. Geologic and geochemical factors controlling uranium, radium-226, and radon-222 in ground water, Newark Basin, New Jersey. In: Gundersen, L.C.S., Wanty, R.B. (Eds.), Field Studies of Radon in Rocks, Soils, and Water, U.S. Geol. Surv. Bull. 1971, pp. 243–265.
Szenknecht, S., Costin, D.T., Clavier, N., Mesbah, A., Poinssot, C., Vitorge, P., Dacheux, N., 2013. From uranothorites to coffinite: a solid solution route to the thermodynamic properties of $USiO_4$. Inorg. Chem. 52, 6957–6968. http://dx.doi.org/10.1021/ic400272s.
Tang, J., Johannesson, K.H., 2003. Speciation of rare earth elements in natural terrestrial waters: assessing the role of dissolved organic matter from the modeling approach. Geochim. Cosmochim. Acta 67 (13), 2321–2339. http://dx.doi.org/10.1016/S0016-7037(02)01413-8.
Tang, J., Johannesson, K.H., 2005. Rare earth element concentrations, speciation, and fractionation along groundwater flow paths: the Carrrizo sand (Texas) and upper Floridan aquifers. In: Johannesson, K.H. (Ed.), Rare Earth Elements in Groundwater Flow Systems. Springer, Dordrecht, pp. 223–252.
Tang, J., Johannesson, K.H., 2006. Controls on the geochemistry of rare earth elements along a groundwater flow path in the Carrizo Sand aquifer, Texas, USA. Chem. Geol. 225, 156–171. http://dx.doi.org/10.1016/j.chemgeo.2005.09.007.
Vinson, D.S., Vengosh, A., Hirschfeld, D., Dwyer, G.S., 2009. Relationships between radium and radon occurrence and hydrochemistry in fresh groundwater from fractured crystalline rocks, North Carolina (USA). Chem. Geol. 260, 159–171. http://dx.doi.org/10.1016/j.chemgeo.2008.10.022.
Wanty, R.B., Schoen, R., 1991. A review of the chemical processes affecting the mobility of radionuclides in natural waters, with applications. In: Gundersen, L.C.S., Wanty, R.B. (Eds.), Field Studies of Radon in Rocks, Soils, and Water, U.S. Geol. Surv. Bull. 1971, pp. 183–194.
Wanty, R.B., Miller, W.R., Briggs, P.H., McHugh, J.B., 1999. Geochemical processes controlling uranium mobility in mine drainage. In: Plumlee, G.S., Logsdon, M.J. (Eds.), The Environmental Geochemistry of Mineral Deposits Part A: Processes, Techniques and Health Issues, Soc. Econ. Geol., Reviews in Economic Geology, vol. 6A, pp. 201–213.
Warner, R., Meadows, J., Sojda, S., Price, V., Temples, T., Arai, Y., Fleisher, C., Crawford, B., Stone, P., 2011. Mineralogic investigation into occurrence of high uranium well waters in upstate South Carolina, USA. Appl. Geochem. 26, 777–788. http://dx.doi.org/10.1016/j.apgeochem.2011.01.035.
Willis, S.S., Johannesson, K.H., 2011. Controls on the geochemistry of rare earth elements in sediments and groundwaters of the Aquia aquifer, Maryland, USA. Chem. Geol. 285, 32–49. http://dx.doi.org/10.1016/j.chemgeo.2011.02.020.
Wood, S.A., 1990. The aqueous geochemistry of the rare-earth elements and yttrium 1: review of available low-temperature data for inorganic complexes and the inorganic REE speciation of natural waters. Chem. Geol. 82, 159–186.
Yang, Q., Smitherman, P., Hess, C.T., Culbertson, C.W., Marvinney, R.G., Smith, A.E., Zheng, Y., 2014. Uranium and radon in private bedrock well water in Maine: geospatial analysis at two scales. Environ. Sci. Technol. 48, 4298–4306. http://dx.doi.org/10.1021/es405020k.
Zänker, H., Hennig, C., 2014. Colloid-borne forms of tetravalent actinides: a brief review. J. Contam. Hydrol. 157, 87–105. http://dx.doi.org/10.1016/j.jconhyd.2013.11.004.